

Zeitschrift: Eclogae Geologicae Helvetiae
Herausgeber: Schweizerische Geologische Gesellschaft
Band: 59 (1966)
Heft: 2

Artikel: Shell microstructure of a planktonic foraminifer, Globorotalia menardii (d'Orbigny)
Autor: Bé, Allan W. H. / McIntyre, Andrew / Breger, Dee L.
DOI: <https://doi.org/10.5169/seals-163398>

Nutzungsbedingungen

Die ETH-Bibliothek ist die Anbieterin der digitalisierten Zeitschriften auf E-Periodica. Sie besitzt keine Urheberrechte an den Zeitschriften und ist nicht verantwortlich für deren Inhalte. Die Rechte liegen in der Regel bei den Herausgebern beziehungsweise den externen Rechteinhabern. Das Veröffentlichen von Bildern in Print- und Online-Publikationen sowie auf Social Media-Kanälen oder Webseiten ist nur mit vorheriger Genehmigung der Rechteinhaber erlaubt. [Mehr erfahren](#)

Conditions d'utilisation

L'ETH Library est le fournisseur des revues numérisées. Elle ne détient aucun droit d'auteur sur les revues et n'est pas responsable de leur contenu. En règle générale, les droits sont détenus par les éditeurs ou les détenteurs de droits externes. La reproduction d'images dans des publications imprimées ou en ligne ainsi que sur des canaux de médias sociaux ou des sites web n'est autorisée qu'avec l'accord préalable des détenteurs des droits. [En savoir plus](#)

Terms of use

The ETH Library is the provider of the digitised journals. It does not own any copyrights to the journals and is not responsible for their content. The rights usually lie with the publishers or the external rights holders. Publishing images in print and online publications, as well as on social media channels or websites, is only permitted with the prior consent of the rights holders. [Find out more](#)

Download PDF: 09.07.2025

ETH-Bibliothek Zürich, E-Periodica, <https://www.e-periodica.ch>

Shell Microstructure of a Planktonic Foraminifer, *Globorotalia menardii* (D'ORBIGNY)¹⁾

by Allan W. H. Bé, Andrew McIntyre, and Dee L. Breger²⁾

With 2 Figures and 1 Table in the text and 17 Plates

ABSTRACT

The surface features of the shell of the modern planktonic foraminiferal species, *Globorotalia menardii* (D'ORBIGNY), have been examined with an electron microscope. Microstructural details have been observed on the keel, chambers, and lip on the apertural side of a complete replica as well as on the spiral and apertural sides of other selected specimens. Maximum crystal size and minimum pore diameters are found on the earlier chambers of the last whorl, whereas minimum crystal size and maximum pore diameters are present on the last-formed chambers. This is the result of primary (bilamellar) shell growth and secondary thickening. Shell thickening is believed to occur in two ways: (a) during normal ontogenetic development of a bilamellar test in the photic zone, and (b) during the adaptation of the individual to greater depth habitats, when a calcite crust of considerable thickness is deposited over the bilamellar shell.

INTRODUCTION

The use of the electron microscope for examining fine structural details in microfossils is comparatively new. During the past decade there have been a number of electron-microscopic investigations of modern and fossil diatoms, coccolithophorids, and molluscs, indicating that skeletal construction and crystallographic features are of taxonomic and ecologic importance. Few such studies have been attempted on the Foraminifera, whose abundance and diversity are truly astounding as witnessed by the total number of fossil and modern species (27,000) and genera (1200) described (LOEBLICH & TAPPAN, 1964). The first publication dealing with electron microscopic examination of the foraminiferal test is one by JAHN (1953). HEDLEY & BERTAUD (1962) studied the cytology and shell of a pseudochitonous species *Gromia oviformis* with an electron microscope. HAY, TOWE, & WRIGHT (1963) introduced the carbon shadow-casting method to foraminiferalogy and analysed microstructures of the tests of various genera and families to determine their taxonomic significance. Such a broad comparative survey requires study on the family or generic level.

The present investigators have taken a narrower approach and made electron microscopic examinations of foraminiferal tests belonging to the planktonic families *Globigerinidae* and *Globorotaliidae* on specific and generic levels (BÉ, 1965). We

¹⁾ Lamont Geological Observatory, Contr. No. 958.

²⁾ Lamont Geological Observatory of Columbia University, Palisades, New York.

wished to see which microstructures are of systematic importance and which ones are influenced by environmental conditions. Our procedure is to describe the main structural features of the individual test and to try relating these observations to their ecological adaptations. As our knowledge of the significance of these microstructural features grows, we shall not only be able to make more precise taxonomic delineations, but also learn about the interrelationships between organic crystal growth and environmental conditions.

METHODS

Since the foraminiferal test is too thick to be viewed directly in an electron microscope, a replica of the surface to be examined must be prepared that is sufficiently thin to be penetrated by the electron beam. This can be done either by the direct one-stage method (HAY, TOWE, & WRIGHT, 1963) or the indirect two-stage method (KAY, 1965; BRADLEY, 1961; KRINSLEY & BÉ, 1965).

In the direct method, a number of specimens are placed on a glass slide with double-stick tape after they have been cleaned ultrasonically in a dilute solution of sodium metaphosphate. The specimens are replicated by shadow-casting at an angle of 30° from the horizontal with platinum-palladium or silicon monoxide and then plated at 90° with carbon in a vacuum-evaporator. They are then placed in a dilute solution of hydrochloric acid for several hours to remove the calcium carbonate. The replica film (ca. 100 Å thick) is transferred onto a fine-mesh copper grid, dried, and viewed in the Philips EM 75C electron microscope used in our study. The direct method yields replicas of higher resolution than can be obtained with the indirect process.

In the indirect method, several cleaned specimens are placed on a strip of acetate film and each moistened with acetone, so that the undersides of the specimens are molded in the acetate. The calcium carbonate is dissolved in a hydrochloric acid solution with ultrasonic agitation. Shadowing and plating of the molds proceeds as described for the direct method. After replication, the molds are cut from the acetate strip, and each replica is placed facing upwards on a 200-mesh grid. The acetate is dissolved slowly by condensation of acetone vapors in a reflux unit, leaving the replica on the grid ready for viewing. The indirect method is preferable for obtaining large replicas because the vigorous action of carbonate removal occurs prior to shadow-casting. Thus the delicate film has a better chance of survival than in the direct process.

The rather flat test of *Globorotalia menardii* is of great benefit in our study because it allows the replica to hold together better than if the specimens are more globular or highly curved. It is difficult to obtain complete, unbroken replicas of an entire side of the foraminiferal test, which is generally too large an object for total-image recording under an electron microscope. Complete replicas are necessary so that structures can be oriented with respect to the whole test and individual chambers. Unfortunately, very often the replica breaks apart and the remaining fragments may not always tell us what part(s) of the shell they represent. When successful, it is best to photograph each portion of the replica that appears on the

200-mesh EM copper grid. This is possible by removing the objective aperture in the Philips EM 75C. By piecing together the individual grid openings, we are able to obtain a mosaic of the replica (Pl. II, Fig. 1), from which we have reconstructed the total outline of the apertural side of the test (Pl. II, Fig. 2). Such a complete replica is obtained rarely and is very useful for later comparison with the higher magnification electron micrographs.

We have also examined with the light microscope the internal structures of planktonic Foraminifera by means of the acetate-peel method (KRINSLEY & BÉ, 1965; BÉ & LOTT, 1964). Lamellar growth lines appear much more distinctly in acetate peels than in conventional thin-sections. Optical examination of internal structures and shell growth is a necessary adjunct to electron microscopy of Foraminifera.

DISTRIBUTION AND SHELL MORPHOLOGY

Globorotalia menardii occurs abundantly in equatorial waters, especially between 20°N and 20°S latitudes of the Atlantic, Pacific, and Indian Oceans, and it is carried towards the middle latitudes by the warm currents (Gulf Stream, Kuroshio, Brazil Currents, etc.) along the eastern margins of the continents (Fig. 1). It appears in lower concentrations in the subtropical central water masses of the oceans, where it is more common during the warmer months of the year. In the Atlantic Ocean, *G. menardii* is transported northeastward by the Gulf Stream and has been encountered in plankton tows as well as in bottom sediments as far as 50°N latitude and 30°W longitude in the region of the Mid-Atlantic Ridge. The specimens for our study came from a bottom sediment sample collected in the central North Atlantic at 35° 06' N and 45° 06' W in 4755 m of water.

The species we have selected for our study is the typical form living in modern seas and belongs to a large evolutionary lineage, including such fossil or living forms as *Globorotalia menardii multicamerata* CUSHMAN & JARVIS, *Globorotalia menardii miocenica* PALMER, *Globorotalia menardii praemenardii* CUSHMAN & STAINFORTH, *Globorotalia menardii unguolata* BERMUDEZ, *Globorotalia menardii* (D'ORBIGNY) var. *fimbriata* (BRADY), *Globorotalia tumida* (BRADY), and *Globorotalia tumida flexuosa* (KOCH). Additional taxonomic complications have arisen with the recent choice of a neotype for *Globorotalia cultrata* (D'ORBIGNY) by BANNER & BLOW (1960), who thereby recommend the suppression of the well-known *Globorotalia menardii*. However, we prefer to employ the name *Globorotalia menardii* instead of *Globorotalia cultrata*, and concur with TODD's (1961, 1963) arguments in this matter.

Globorotalia menardii (Fig. 2 and Pl. I, Fig. 1) is characterised by its rather flat, biconvex test with a prominent, bulging keel. The mature tests used in this study ranged in length-width dimensions from 1000 $\mu \times$ 850 μ to 1200 $\mu \times$ 950 μ . Every whorl is normally composed of 5 to 6 angular-rhomboid chambers, which are clearly delineated from one another by depressed sutures on the apertural side and remnant (septal) keels on the spiral side. The coiling direction is almost exclusively to the left, although during the Pliocene this species was dextrally coiled (ERICSON, EWING & WOLLIN, 1963).

The surface texture is relatively smooth in comparison to most of the other planktonic foraminiferal species. But, as we shall note later, surface topographic features of the shell can to a large extent be a function of the total age of the individual specimen as well as the recency of each chamber formation. The conventional descriptions of the shell have noted a range from smooth to hispid or «spinose» texture, with coarsening being particularly evident near the apertural and umbilical regions. The term «spinose» for the coarse crystallinity of the pustules in *Globorotalia menardii* is misleading because it should only be applied to the true, elongate spines present among species of *Globigerinoides*, *Orbulina*, and *Globigerina*.

The shells of planktonic Foraminifera are composed of calcite crystals, whose c- and major growth axes are oriented normal to the shell surface. In cross section the radial structure of the walls is quite evident, but we have not yet studied the entire crystal units that constitute the walls to determine their crystallographic habit. We can only state that the crystals appear from qualitative inspection to be of the rhombohedral form, of which three rhombic faces are exposed to give the surface expression of three-sided pyramids – henceforth referred to as rhombic crystals in the text. «Crystal size» is expressed as the maximum length from one end of the intersection of two faces to the base of the third face (Plate XI).

The structural development of the shell can best be followed by studying the surface and internal features of the chambers. Each chamber represents an «instar» or increment of growth, during which two lamellae are added to the test. The inner lamella is limited to the individual chamber, while the outer lamella is deposited over this chamber as well as over the whole previously formed shell (REISS, 1957, 1958, 1963a, b). The bilamellar secretory process causes progressive thickening of the earlier chambers but, from our observations of a closely related species, *Globorotalia truncatulinoides* (D'ORBIGNY), this does not add a substantial amount to the total test thickness (BÉ & ERICSON, 1963; BÉ & LOTT, 1964). On the other hand, we believe that an additional process yields very considerable calcification over the original, bilamellar test as the organism descends from the euphotic zone and adapts itself to increasingly deeper habitats well below 500 m (BÉ, 1965). We have estimated that this secondary thickening or «calcite crust» can amount to twice the thickness of the original shell. It frequently coats the chambers of the last whorl of mature tests and their wall thickness contrasts sharply with the thin walls of the inner chambers of earlier ontogenetic stages (Pl. I, Figs 2 and 3).

Since each chamber grows progressively thicker due to bilamellar and calcite crust deposition, we can consider the five chambers in the last whorl of *G. menardii* as sequential stages (Fig. 2). The final or fifth chamber is stage 1, the penultimate or fourth chamber is stage 2, and so forth.

One of the major difficulties we have encountered in interpreting our electron-micrographs is the finding of criteria to distinguish between first-order features and second-order microstructural variations due to developmental phases and/or environmental influences. We consider the poreless keel and apertural lip of *Globo-*

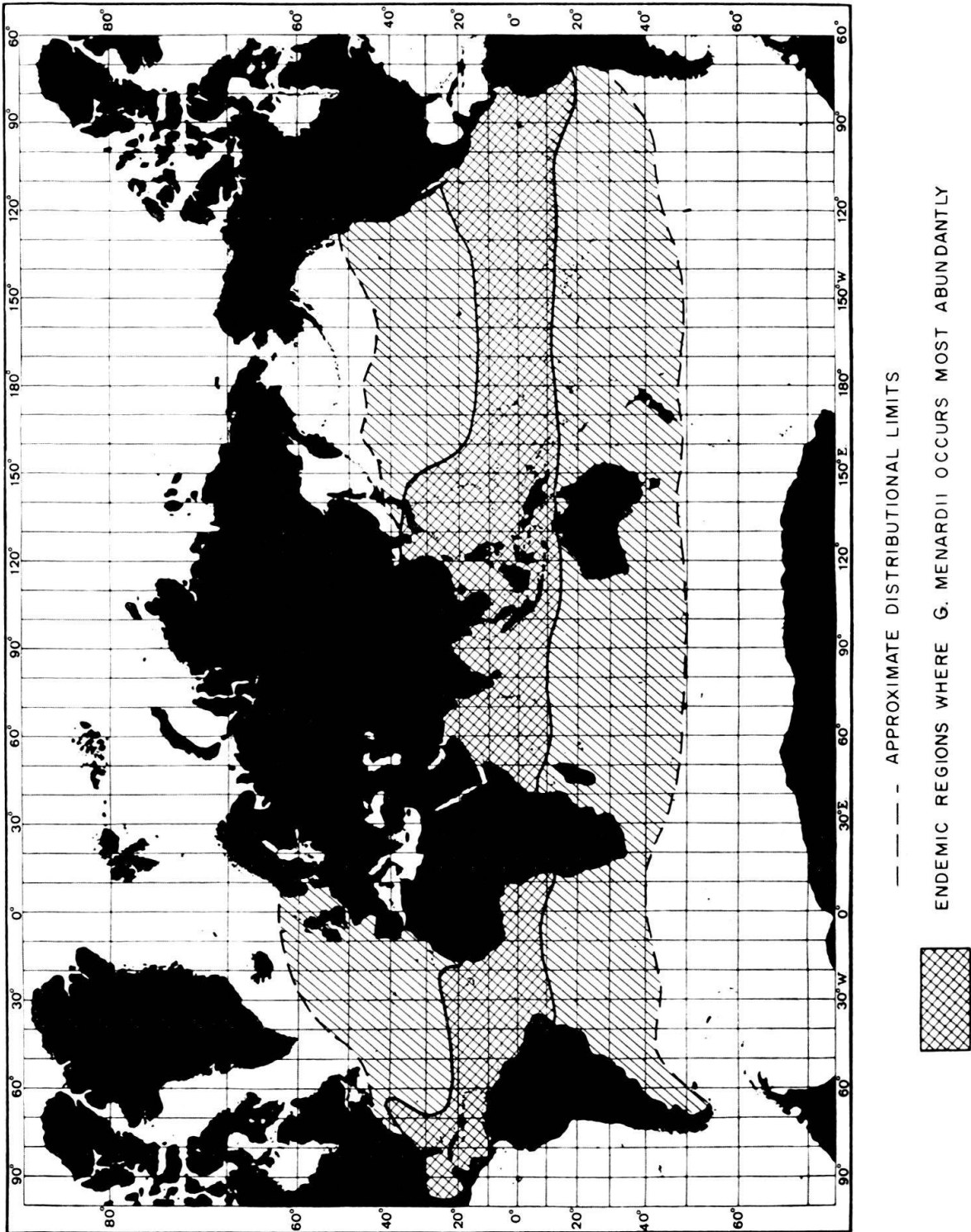


Fig. 1. Geographic distribution of *Globorotalia menardii*. Endemic regions (cross-hatched) are in tropical waters. Seasonal variations in abundance occur in subtropical waters (oblique lines).

rotalia, and the size and shape variations and distributional patterns of pores in all species as first-order features. Spines and spine bases in *Globigerinoides*, *Orbulina*, and *Globigerina* also should fall in this category as well as linear and radial (ornamental?) patterns on the shell surface.

We recognise as second-order features those that apparently have developed subsequent to the gross structures, and which may have been produced during adaptation to certain ecological conditions. One such type is the pustules (knobs, tubercles, papillae) or local prominences that are characteristically present along the apertural-umbilical region in most species of *Globorotalia*. Another is the increase in crystal size and corresponding decrease in pore diameters in the earlier chambers. The question that is still unresolved is: How much do ontogenetic development and/or adaptation to bathypelagic habitat contribute to the test thickening (and accompanying increase in crystal size)?

In the following discussion, we have arranged the electron micrographs in such a manner that Plates III–VIII are from the apertural side of a single specimen of *G. menardii*; Plates IX–XI illustrate the keel on the apertural side of various specimens; Plates XII–XIV represent chambers on the apertural side of different, selected specimens; and Plates XV–XVII depict the spiral side of other miscellaneous specimens. The reader should refer to Fig. 2 for the conventional terms used in describing some of the morphological features on the foraminiferal test. Morphological variability and aberrancies complicate a study such as ours, particularly when it is based on few specimens examined at high magnifications. Future studies along these lines will certainly provide additional details to our present, limited observations.

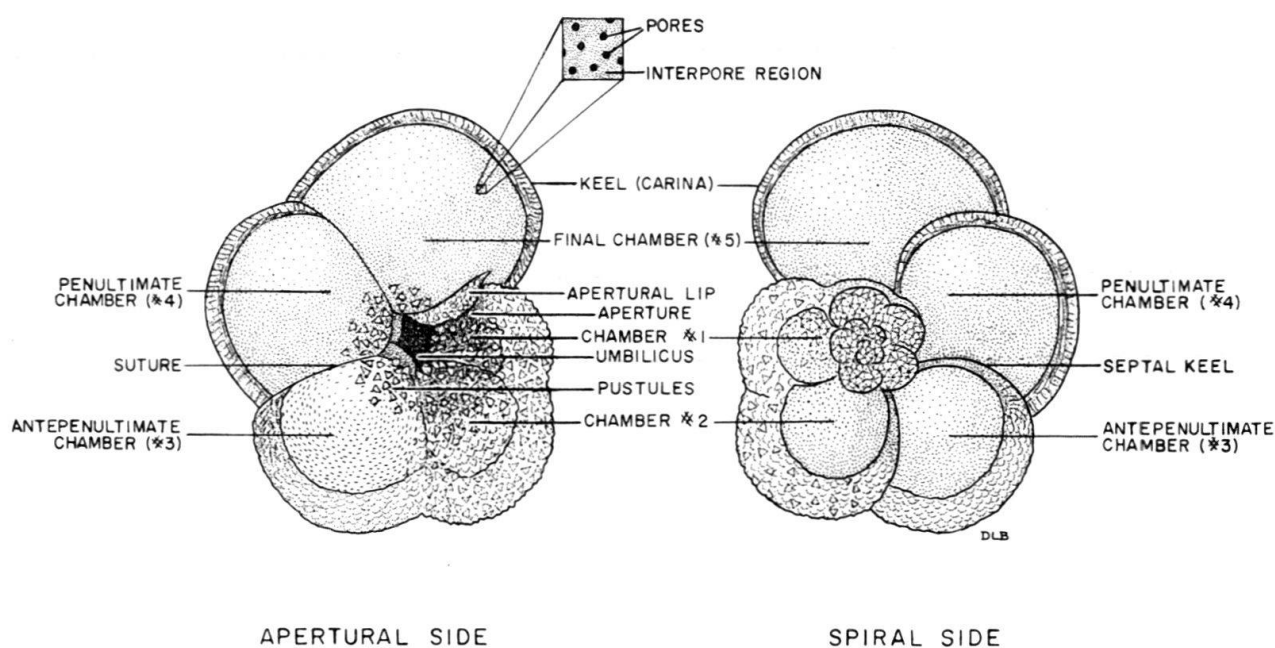


Fig. 2. Apertural and spiral sides of *G. menardii* with morphological terms used in text.

1. Microstructures of the keel (carina)

This is the non-porous peripheral region, varying in mature specimens from 50 to 100 μ and averaging 80 μ in width, depending on shell size and the degree of crystalline thickening. It is a distinguishing character of the family *Globorotaliidae*, and although not all species in this family possess a keel, it is exemplified in *G. menardii*.

The development of the keel can be traced by examining each chamber, from the youngest to the oldest chamber of the last whorl of our complete replica (Pls. III–VIII) and from other selected specimens (Pls. IX–XVII).

On Chamber 5, the transition from the porous chamber to the keel proper is gradual and often marked by linear ridges composed of microcrystals less than 1 μ in size. They are generally oriented obliquely (Pl. III, Fig. 2; Pl. XIII, Fig. 1; Pl. XV, Fig. 2) or parallel (Pl. IX, Fig. 2) at the inner edge. Towards the periphery, the structures are elongated or equidimensional, rounded prominences built by larger crystals, some of which possess smooth faces (Pl. III, Fig. 2; Pl. IX, Fig. 2; Pl. XVII). At this early stage, the microcrystals have a seemingly random orientation (Pl. IX, Fig. 1), which at closer examination reveals three preferred directions. Some of these small crystals form the bases of the subsequent, large euhedral crystals (Pl. V, Fig. 2; Pl. XI).

On Chamber 4, the keel develops a coarser texture due to increased growth in crystal size. Discrete knobs or roughly circular units (5–8 μ in diameter) are visible, composed of interlocking subhedral crystals (2–5 μ) with many growth steps on the crystal faces (Pl. IV, Fig. 1; Pl. X, Fig. 3). The gross rhombic shapes of the incompletely formed crystals are starting to become evident.

On Chambers 2 and 3, the keel is coarsely crystalline and maximum crystal size is probably reached in Chamber 1. The trend is clearly towards further development of the growth steps (Pl. XI, Fig. 1), until euhedral crystals with perfect rhombic shapes and smooth faces are attained (Pl. V, Fig. 2; Pl. XI, Fig. 2). The euhedral crystals, forming this so-called calcite crust, are generally larger than on the porous regions of the chambers. They vary widely in size, with a maximum dimension of 20 μ and averaging around 10 μ .

2. Microstructures of apertural lip

The aperture is an elongated opening, bordered by a non-porous «lip» that protrudes over Chamber 1. The concentration and size of the protuberances on the lip as well as the lip's shape vary a great deal from specimen to specimen. Because of its proximity to the umbilicus and the apertural void, the lip region is difficult to replicate and, hence, our data are based on limited observations (Pl. VIII, Fig. 1).

The transitional region from porous chamber to the lip proper is again marked by a band (about 13 μ wide) of linear ridges parallel to the rim. The rhombic crystals (2 μ) are intermediate in size between the porous chamber and lip. On the lip itself, the rhombic crystals vary widely in size and probably reach a maximum of 12 μ .

3. Microstructures of chambers

Except for the relatively small areas of the keel and apertural lip, the rest of the shell is penetrated by thousands of pores. Variations in the size, shape, concentration, and distributional patterns of pores have not been generally evaluated because their examination is rather tedious and their significance unproved. Yet, several authors have shown their potential value in classification, paleoecology, and tracing evolutionary lineages. HOFKER (1951, 1956) has pointed out that foraminiferal species with smaller pores (protopores) are more primitive and are precursors of the more advanced forms having larger pores with diameters greater than $2\ \mu$ (deuteropores). He introduced the «pore-index» measurement, which, for example, can be expressed as $7-1.5, \times 500$. This indicates an average of seven pores with average diameter of $1.5\ \mu$ per cm^2 , at a magnification of $\times 500$ (or 7 pores, with $3\ \mu$ diameter, in a $20 \times 20\ \mu$ square, at actual size). HOFKER (1956) listed the following pore-indices for some planktonic Foraminifera:

<i>Globorotalia fimbriata</i> (BRADY)	14- $1\frac{1}{2}$
<i>Globorotalia tumida</i> (BRADY)	12- $1\frac{1}{2}$
<i>Globigerina eggeri</i> RHUMBLER	
[<i>Globoquadrina dutertrei</i> (D'ORBIGNY)]	10- $1\frac{1}{2}$
<i>Globorotalia menardii</i> (D'ORBIGNY)	10-1
<i>Globigerina quinqueloba</i> NATLAND	5-1
<i>Orbulina universa</i> D'ORBIGNY	8-1
<i>Globigerinoides ruber</i> (D'ORBIGNY)	5- $1\frac{1}{2}$
<i>Globigerina digitata</i> BRADY	7-2
<i>Globigerinella aequilateralis</i> (BRADY)	$4\frac{1}{2}$ -3
<i>Globigerina bulloides</i> D'ORBIGNY	3- $3\frac{1}{2}$
<i>Globigerinoides conglobatus</i> (BRADY)	3- $3\frac{1}{2}$
<i>Globigerinoides sacculifer</i> (BRADY)	3- $3\frac{1}{2}$
<i>Sphaeroidinella dehiscens</i> (PARKER & JONES)	$1\frac{1}{2}$ -5.6

The list shows that the relatively smooth-shelled *Globorotalia* has a higher density of pores with smaller diameters than *Globoquadrina* or *Globigerina*, while the spinose, coarsely textured *Globigerinoides* and *Sphaeroidinella* possess the lowest concentration of pores with the biggest diameters. Although the pore-index is a constant feature within a species, there may be some variation due to ontogeny.

BERGGREN (1960) has also demonstrated variations in the concentration, pattern, and diameters of pores between six recent planktonic foraminiferal species from the Gulf of Mexico. He found a wide range of variation from species with a large number of pores per unit area and small pore diameters (i.e. *Globorotalia menardii*) to species with a small number of pores per unit area and large pore diameters (i.e. *Globigerinoides sacculifer*). *Globigerinoides ruber* (D'ORBIGNY), *Globigerina eggeri* RHUMBLER, *Globigerinoides conglobatus* (BRADY), and *Globigerina bulloides* D'ORBIGNY fall between these extremes.

Pores may vary considerably also in shape. BERGGREN (1960) observed that they are rarely geometrically circular; they are more commonly subcircular, oval, or elliptical in outline. We found that species having larger pores, e.g. *Globigeri-*

noides sacculifer or *Orbulina universa* tended to have irregular shapes, whereas the fine-pored species (e.g. *Globorotalia menardii*) were relatively circular and cylindrical.

Several authors have also noted that certain regions of the foraminiferal test tended to be imperforate or less perforate, such as the keel (carina), apertural area, septa, apertural lips, umbilical plates or teeth, and along «ornamental» regions (ridges, costae, pustules, knobs).

Pore concentration appears to be affected by environmental changes according to Wiles's study (in press) of the pore concentration of *Globigerina eggeri* RHUMBLER in Pacific deep-sea cores. He presented convincing evidence that changes in pore concentration can be correlated with Pleistocene temperature variations, as determined independently both by faunal analyses and oxygen-isotope ratios. His results indicated that high pore counts per unit area occurred during interglacial times and low counts per unit area represented glacial periods.

These few studies have already shown the importance of pores as conservative features within any given species. Their significance and role in ecology, paleoecology, and evolution remain to be examined more carefully.

In the following discussion, we shall note that the pores are intimately linked with changes in the test wall. As we trace the effects of lamellar thickening in successively earlier chambers, there is corresponding reduction in pore openings. In Chamber 5 of *G. menardii*, the pores are relatively large and open, averaging about 3μ in diameter. There are about 12 to 15 pores per $25 \times 25 \mu$ square and the pores are cylindrical in shape and about 12μ long (Pl. XII, Fig. 2; Pl. XIV, Fig. 6). Close to the inner rim of the keel, two size classes of pores are present. The larger pores are rimmed by circular depressions (Pl. XII, Figs. 1, 3). The transition from the porous chamber to the keel is marked by constrictions of the pores. The crystals that make up the wall material between the pores are scarcely discernible at $\times 1500$ magnification (Pl. III, Fig. 1; Pl. XII, Fig. 2), but at $\times 11,500$ magnification (Pl. XII, Fig. 1) the microcrystals measure about 0.2μ in size.

Chamber 4 shows little or no reduction in the pore diameter, except towards the umbilicus and keel regions, where crystal growth is taking place. Pore diameters vary from about 3.3 to 1.6μ in the central area of the chamber (Pl. IV, Fig. 2; Pl. XIV, Fig. 1). Crystalline growth in the interpore region is evident in the appearance of distinct rhombic crystals of about 0.4 to 1.0μ size (Pl. XIV, Fig. 1). This produces a rougher topography and, hence, coarser texture than in Chamber 5.

Chamber 3 displays a dramatic increase in crystal size over its entire surface in comparison with Chamber 4. Rhombic crystals, from 2 to 10μ diameter, cover the surface of the chamber and greatly obscure the pores (Pl. XIV, Fig. 2; Pls. V and VI). Many pores are choked off and those remaining are reduced in diameter (2μ). The crystals on the keel, however, are larger yet than those on the chamber proper (Pl. V).

Chambers 2 and 1 indicate continuation of growth and attainment of maximum crystal size. Again the crystals vary widely in size, mostly between 7 and 10μ (Pl. VII, Fig. 1). Close to the umbilicus and the aperture the crystals reach a maximum of about 15 to 18μ (Pl. VII, Fig. 2; Pl. VIII, Fig. 2) and except for the

keel region, they are larger here than on any other part of the test. Along the umbilical and apertural regions, the pores have disappeared completely (Pl. VII, Fig. 2). In the central area of Chamber 2, about half of the pores have been obliterated, and few constricted pores (1.3μ diameter) are still visible (Pl. VII, Fig. 1; Pl. XIV, Figs. 3 and 4). The latter are bounded by the bases of 3 or 4 calcite rhombs.

Table 1 presents summarized data on the crystal size and pore dimensions for each of the 5 chambers. The ability to measure the minimum size of the crystals is of course a function of the magnification of the electron micrographs. The table does not take into account the coarser texture around the umbilical area of all the chambers, where large pustules (up to 15μ) are built by single or aggregate crystals.

Table 1. Measurements of crystal size and pores on the apertural side of a single specimen of *Globorotalia menardii* (D'ORBIGNY)

	Crystal size* (μ)			Pore diameter (μ)			Pore Concentration No. of pores/ $25 \mu \times 25 \mu$	Pore length
	Min.	Max.	Mean	Min.	Max.	Mean		
Chamber 1	2	18	10	Many reduced to < 1.3			?	?
Chamber 2	2	16	10	Many reduced to < 1.3			5	?
Chamber 3	2	10	5	1.2	4.0	< 2.0	10	?
Chamber 4	0.4	1.4	1	1.6	3.3	3.0	13-14	12-16
Chamber 5	< 0.1	0.4	0.2	2.2	4.5	3.0	13	16
Keel of Chamber 1	2	16	14					
Keel of Chamber 2	2	15	12					
Keel of Chamber 3	2	13	10					
Keel of Chamber 4	2	5	4					
Keel of Chamber 5	0.5	2	< 1					
Apertural lip	1	12	4					

* Measurement explained on page 888, paragraph 2.

CONCLUSIONS

The keel, apertural lip, and interpore areas on the shell surface of *Globorotalia menardii* possess distinct microstructural features that can best be studied with the electron microscope. These structures can be differentiated from each other on a single chamber, but more spectacular contrasts are evident in the microstructures between adjacent chambers.

We note in mature specimens (> 1 mm long) that successively older (earlier) chambers of the last whorl exhibit progressive shell thickening and a corresponding increase in crystal size. By tracing the structural development from the youngest to the oldest chamber on the apertural side of *G. menardii*, we are able to follow the sequential stages in shell thickening. Chamber 5 is characterised by a relatively smooth keel with linear ridges composed of small crystals, smooth interpore regions built of even smaller crystals ($< 0.1 \mu$), and tubular pores with large diameters

(ca. 3 μ). In Chamber 4 coarsening of the texture of the shell wall is visible in the keel's rounded prominences constructed by aggregates of larger, interlocking crystals with prominent growth steps and, to a lesser extent, in the interpore region. In Chamber 3 and the next two earlier chambers, a sharp increase in crystal growth covers their surfaces with large, euhedral crystals (ca. 10 μ) with smooth faces and which ultimately constrict or obliterate the pore openings. Shell thickening occurs at the expense of pores, whose original concentration is probably uniform for all chambers of the last whorl, but is reduced in the earlier chambers as the pores are gradually filled in by rhombic crystals. Maximum crystal size is attained along the apertural, umbilical, and keel regions of the first and second chambers. Large euhedral crystals with smooth crystal faces are more commonly found on the spiral side as well as along the outer edge of the keel, whereas crystals with growth steps are more prevalent on the apertural side.

We believe that secondary shell thickening in *G. menardii* is due to secretion of a thick calcite crust over its original bilamellar test and that this takes place as the organism descends from the eupotic zone to depths below 500 m. Shell thickening at considerable depths in adult stages of planktonic Foraminifera seems to be a common phenomenon, as it occurs in *Globorotalia truncatulinoides* (BÉ & ERICSON, 1963; BÉ & LOTT, 1964), *Globigerinoides sacculifer* (BÉ, 1965), and other species. One intriguing possibility is that a correlation may be established between maximum crystal size and water depth at which these crystals are formed.

The present study has raised more questions than it has answered. We do not know to what extent shell thickening is due to normal, ontogenetic development or adaptation to a meso-bathypelagic habitat or both. The significance of the microstructural fabrics, the crystal size distribution and patterns and their eventual application to species or generic differentiations, and their utility as ecologic indicators are fruitful fields of investigation that require further attention of micropaleontologists.

ACKNOWLEDGEMENTS

We gratefully acknowledge the aid of Miss Liselotte Schulz in the early stages of our investigation and the helpful discussions with Drs. Marion Jacobs, David Krinsley, Robert Pfister, Tsunemasa Saito and Taro Takahashi. This study received support from the National Science Foundation (Grant GB-4219 and GP-4768).

REFERENCES

- BANNER, F. T. & BLOW, W. H. (1960): *Some primary types of species belonging to the superfamily Globigerinaceae*. Contr. Cushman Found. Foram. Res. 11/1, 1-41.
- BÉ, A. W. H. (1965): *The influence of depth on shell growth in Globigerinoides sacculifer* (BRADY). Micropaleont. 11/1, 81-97.
- BÉ, A. W. H. & ERICSON, D. B. (1963): *Aspects of calcification in planktonic Foraminifera*. In: «Comparative Biology of Calcified Tissues.» N.Y. Acad. Sci., Trans., 109/1, 65-81.
- BÉ, A. W. H. & LOTT, L. (1964): *Shell growth and structure of planktonic Foraminifera*. Science 145, No. 3634, 823-824.
- BERGGREN, W. A. (1960): *Some planktonic Foraminifera from the Lower Eocene (Ypresian) of Denmark and Northwestern Germany*. Stockh. Contr. Geol. 5/3, 41-108.
- BRADLEY, D. E. (1961): *Replica and shadowing techniques*. In: «The Encyclopedia of Microscopy,» G. L. Clark, edit. Reinhold Publ. Corp., New York, p. 229-239.

- ERICSON, D. B., EWING, M. & WOLLIN, G. (1963): *Pliocene-Pleistocene boundary in deep-sea sediments*. Science 139 no. 3556, 727-737.
- HAY, W. H., TOWE, K. & WRIGHT, R. (1963): *Ultramicrostructure of some selected foraminiferal tests*. Micropaleont. 9/2, 171-195.
- HEDLEY, R. H. & BERTAUD, W. S. (1962): *Electron-microscopic observations of Gromia oviformis (Sarcodina)*. J. Protozool. 9/1, 79-87.
- HOFKER, J. (1951): *The Foraminifera of the Siboga Expedition, Pt. III. Ordo Dentata, Sub-ordines Protoforaminata, Biforaminata, Deuteroforaminata*. Monogr. Siboga Exped. 4a, 513 pp.
- (1956): *Foraminifera dentata: Foraminifera of Santa Cruz and Thatch Island, Virginia Archipelago, West Indies*. Spolia Zool. Musei Hauniensis, Univ. Zool. Mus., København, Skrifter 15, 1-237.
- JAHN, B. (1953): *Elektronenmikroskopische Untersuchungen an Foraminiferenschalen*. Zeitschr. Wissensch. Mikroskopie 61/5, 294-297.
- KAY, D. H. (editor) (1965): *Techniques for electron microscopy*. Second edit., 560 pp., F. A. Davis Co., Philadelphia.
- KRINSLEY, D. & BÉ, A. W. H. (1965): *Electron microscope examination of internal structures of Foraminifera*. In: «Handbook of Paleontological Techniques», Kummel, B. & Raup, D., editors. Paleont. Soc., W. H. Freeman & Co., San Francisco, Calif., pp. 335-343.
- LOEBLICH, A. R., Jr. & TAPPAN, H. (1964): *Foraminiferal facts, fallacies, and frontiers*. Geol. Soc. Amer., Bull. 75, 367-392.
- REISS, Z. (1957): *The Bilamellidae, nov. superfam., and remarks on Cretaceous Globorotaliids*. Cushman Found. Foram. Res., Contr. 8/4, 127-145.
- (1958): *Classification of lamellar Foraminifera*. Micropaleont. 4/1, 51-70.
- (1963a): *Note sur la structure des Foraminifères planctoniques*. Revue Micropaléont. 6/3, 127-129.
- (1963b): *Reclassification of perforate Foraminifera*. Ministry of Development Geological Survey Israel, Bull., no. 35, 111 pp.
- TODD, RUTH (1961): *On selection of lectotypes and neotypes*. Cushman Found. Foram. Res., Contr. 12/4, 121-122.
- (1963): *Nomenclature of Foraminifera*. Cushman Found. Foram. Res., Contr. 14/3, 109-111.
- WILES, W. W. (in press). *Pleistocene changes in the pore concentration of a planktonic foraminiferal species from the Pacific Ocean*. In: Sears, M. (edit.) «Progress in Oceanography; Vol. 4: Quaternary History of the Ocean Basin», Proc. 7th Int. Quat. Congress, 1965.

Manuscript received March 31, 1966

Plate I

Fig. 1. Apertural (umbilical) side of *Globorotalia menardii* (D'ORBIGNY).

Fig. 2. Detail of outer shell wall, showing lamellar growth and the extra thick last lamella or «calcite crust» (arrow) (Acetate peel).

Fig. 3. Vertical section through last three chambers and proloculus of *G. menardii*, but not through umbilicus. The thick last lamella or «calcite crust» (arrow) is believed to be secreted as the organism descends from the euphotic zone to great depths. The black, circular objects are air bubbles (Acetate peel).

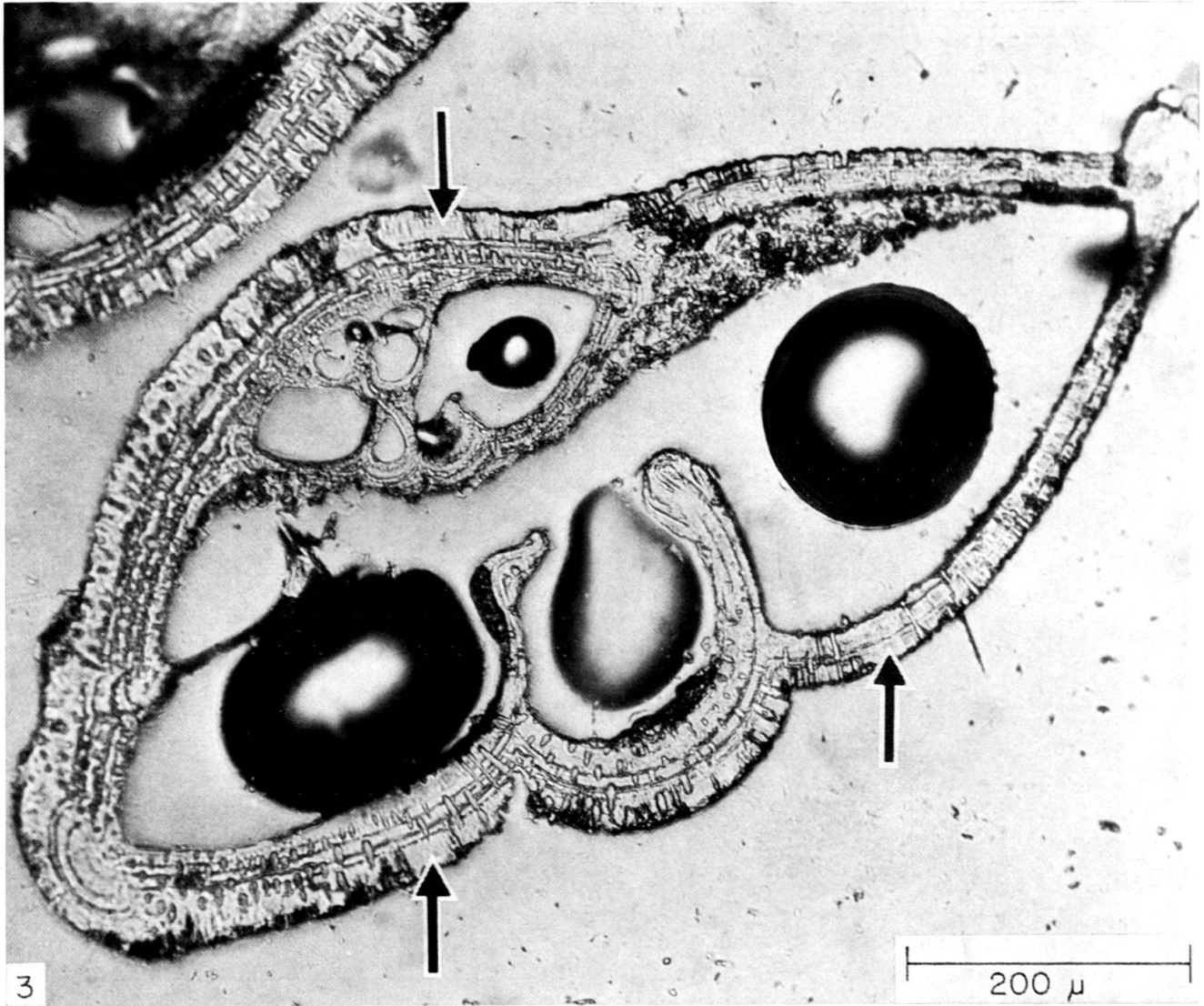
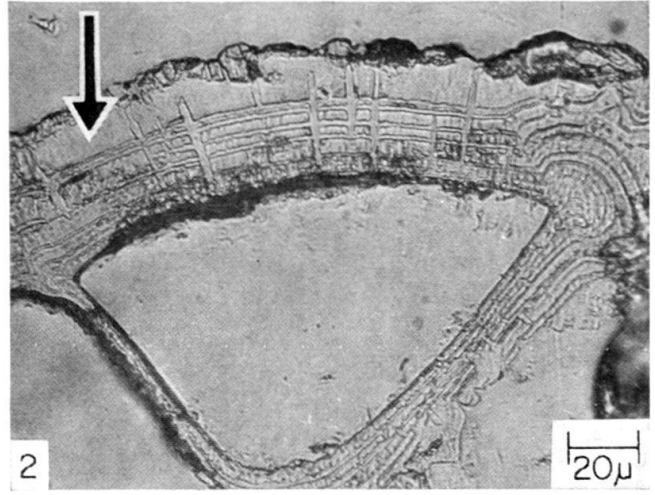
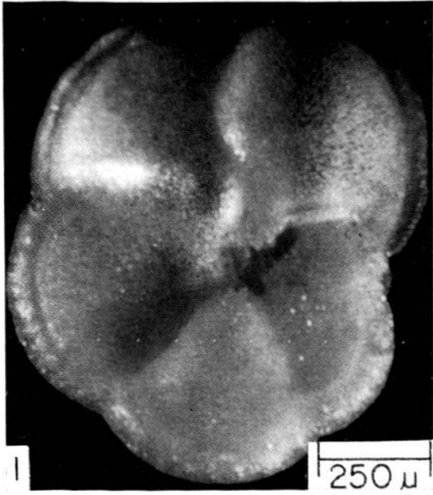
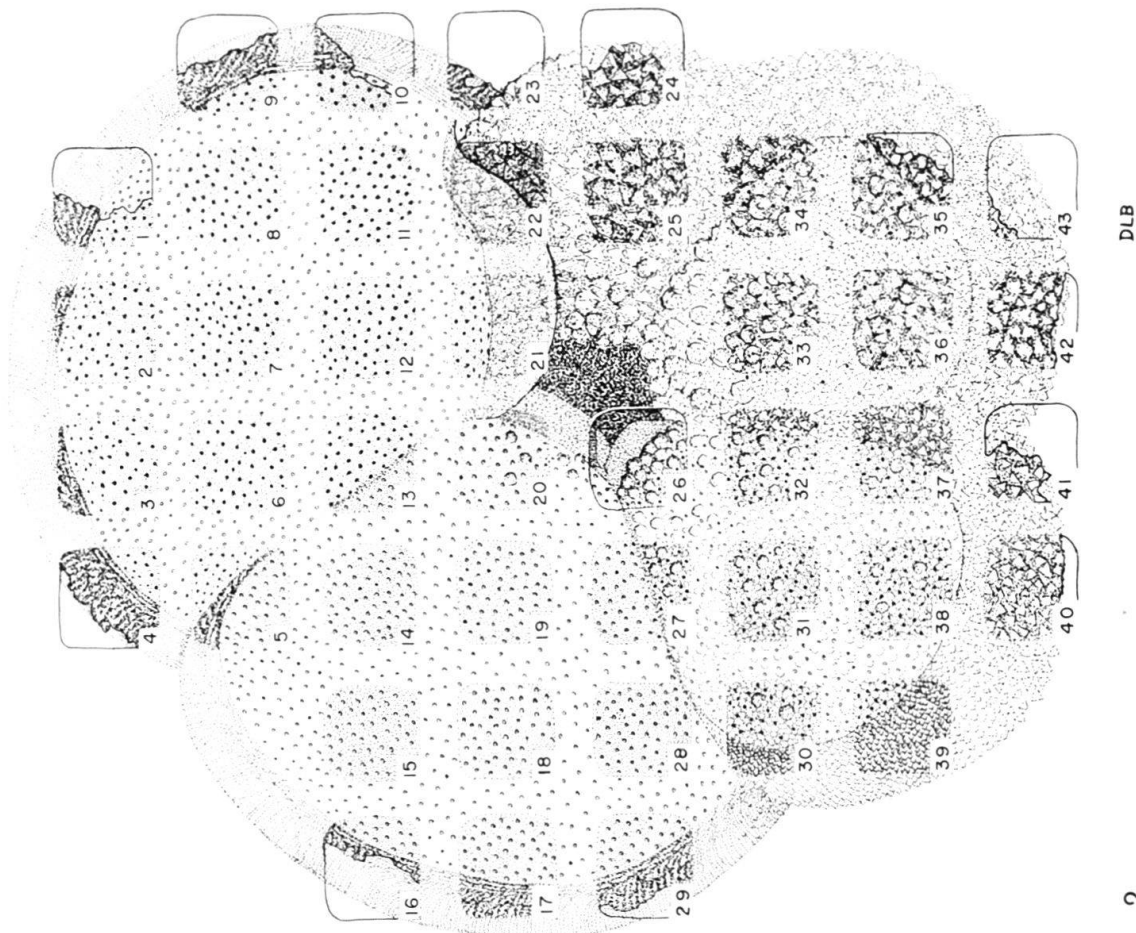


Plate II

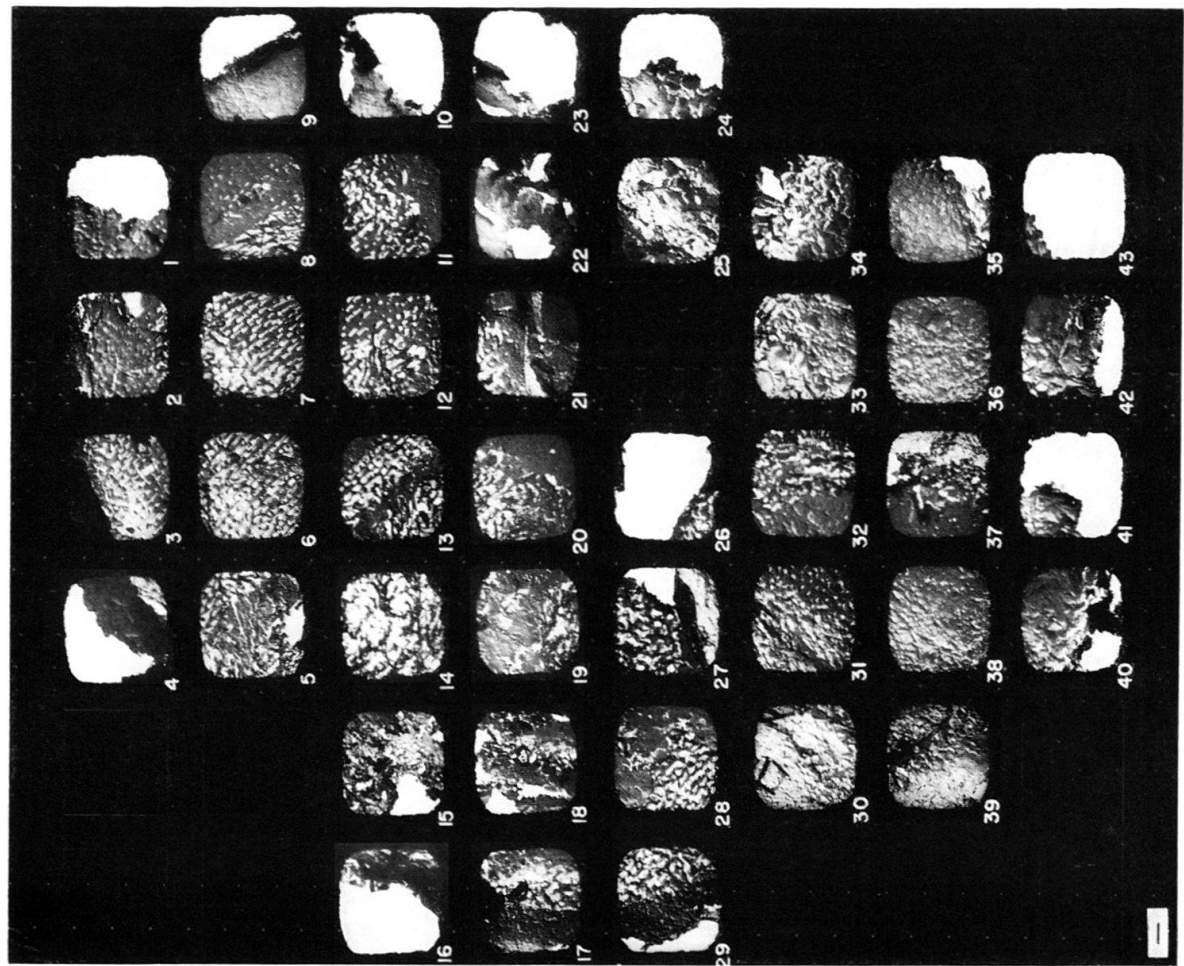
Fig. 1. Mosaic of apertural side of *G. menardii*, made by piecing together electron-micrographs of a single replica showing through individual openings of electron-microscope grid. Each grid opening measures roughly $80\ \mu$ by $80\ \mu$.

Fig. 2. Reconstruction of Fig. 1.



DLB

2



All electron micrographs on Plates III–VIII are from a single specimen (prepared by two-stage replication) and numbered squares refer to those in Plate II. Magnifications are indicated by bar scale.

Plate III

Fig. 1. Chamber 5 with regular pores (Square 7 in Plate II).

Fig. 2. Keel of Chamber 5 (Square 9 in Plate II). Note linear structures with oblique trend.

Fig. 3. Chamber 5 with pores of restricted diameters towards keel region (upper right) (Square 8 in Plate II). Dark tubes are pores which were replicated in two-stage process and which subsequently have collapsed on the replicated surface.

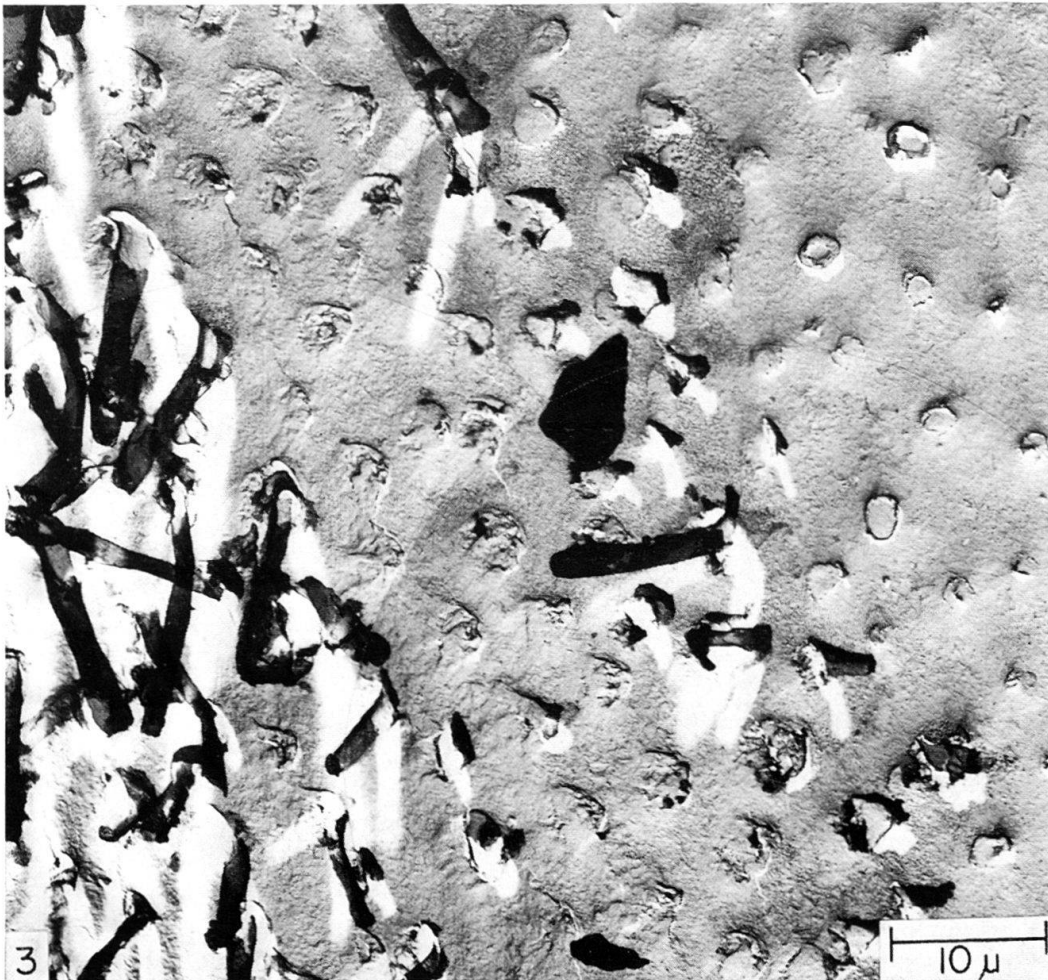
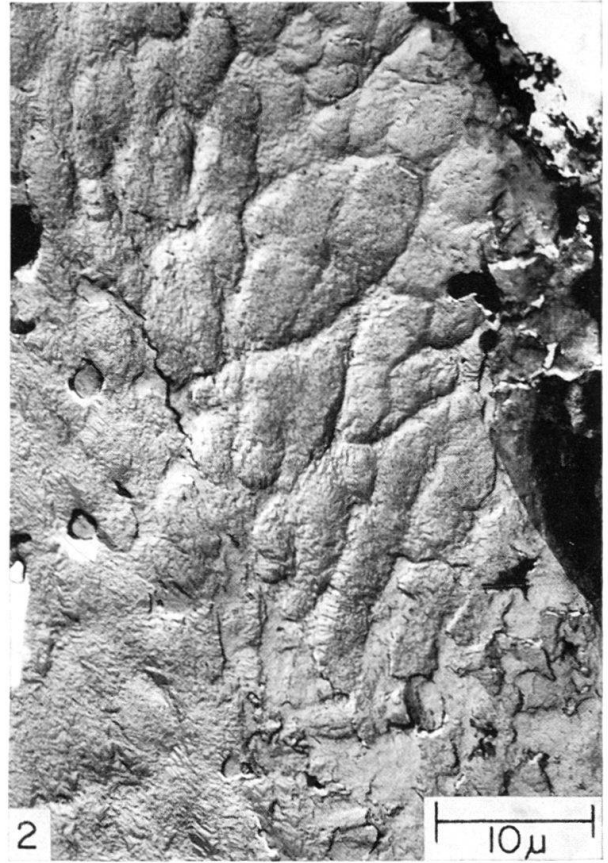
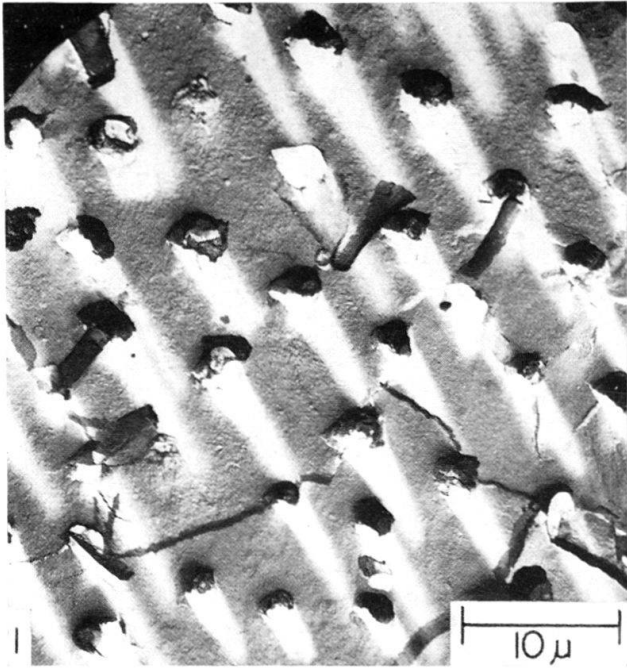


Plate IV

Fig. 1. Keel of Chamber 4 with poreless keel to left and porous chamber to right (Square 29 in Plate II).

Fig. 2. Chamber 4 with pores (lower left part of Square 28 in Plate II).

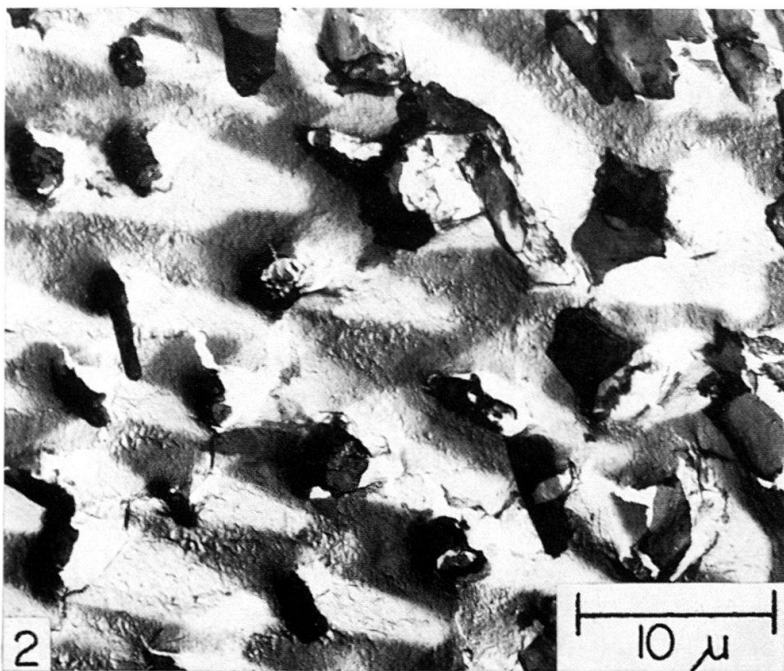
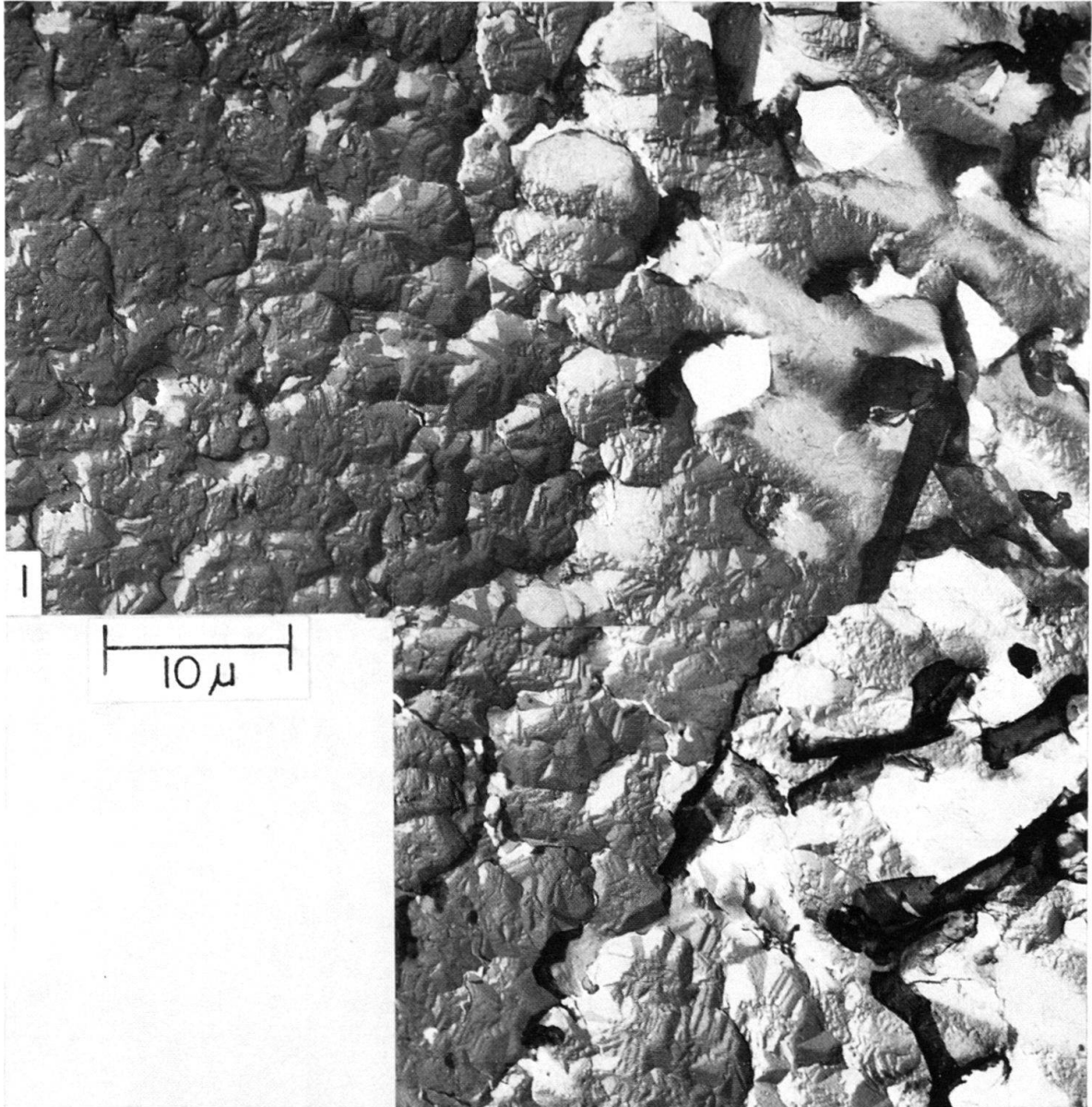


Plate V

Fig. 1. Chamber 3 with large crystals obscuring the pores (arrows) (Square 38 in Plate II).

Fig. 2. Keel of Chamber 3, showing marked increase in size of rhombic crystals (Square 40 in Plate II).

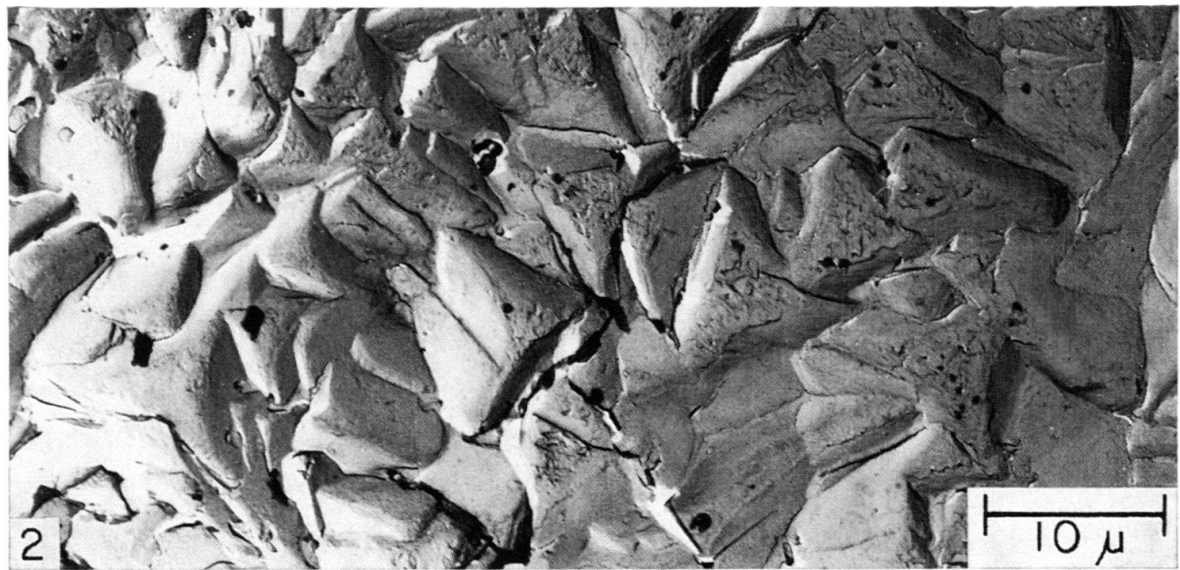
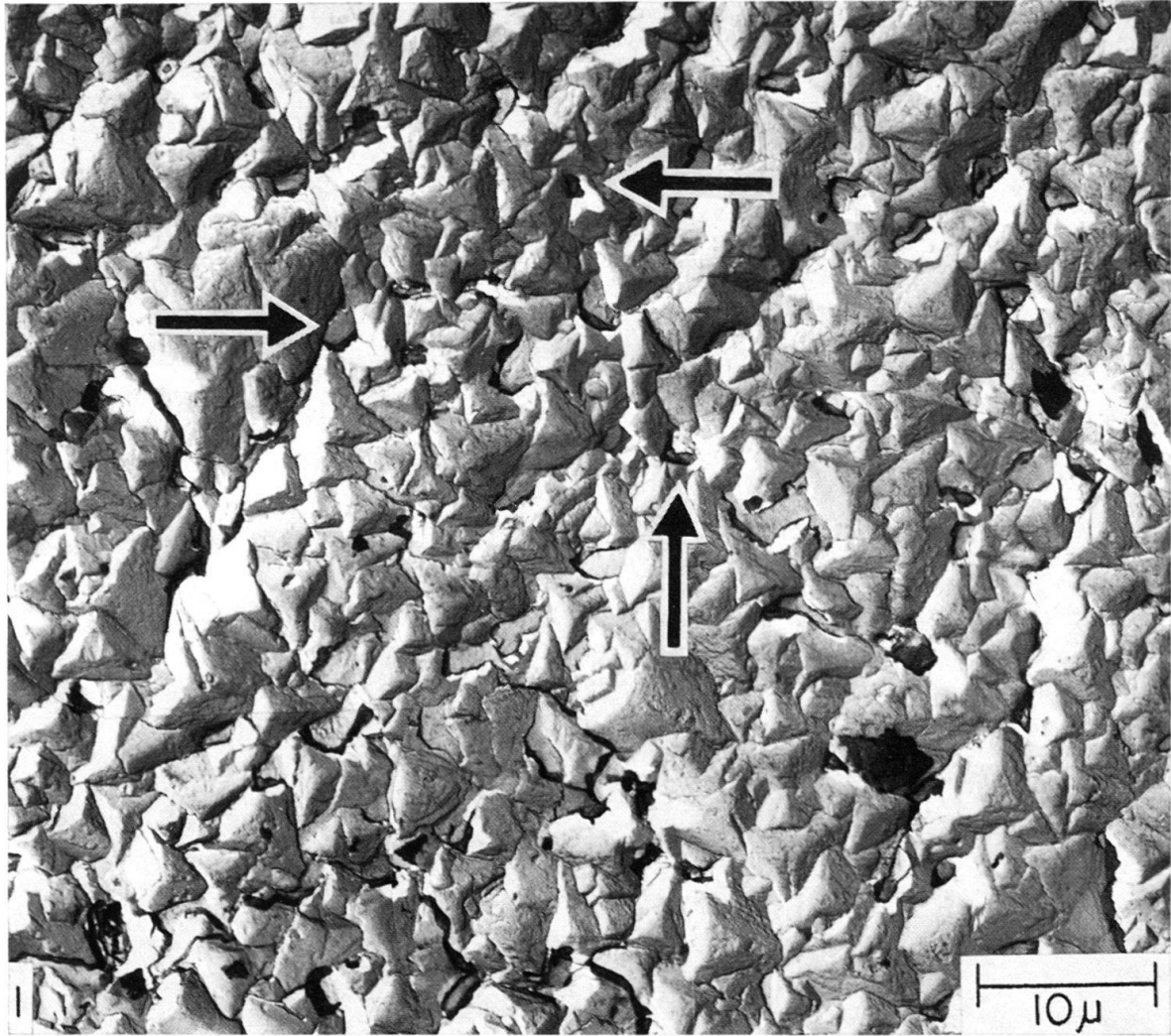


Plate VI

Fig. 1. Septal edge of Chamber 3 (Square 27 in Plate II).

Fig. 2. Chamber 3 with large crystals making up the interpore regions. The trench running obliquely in the upper left is an artifact developed during replication (Square 31 in Plate II).

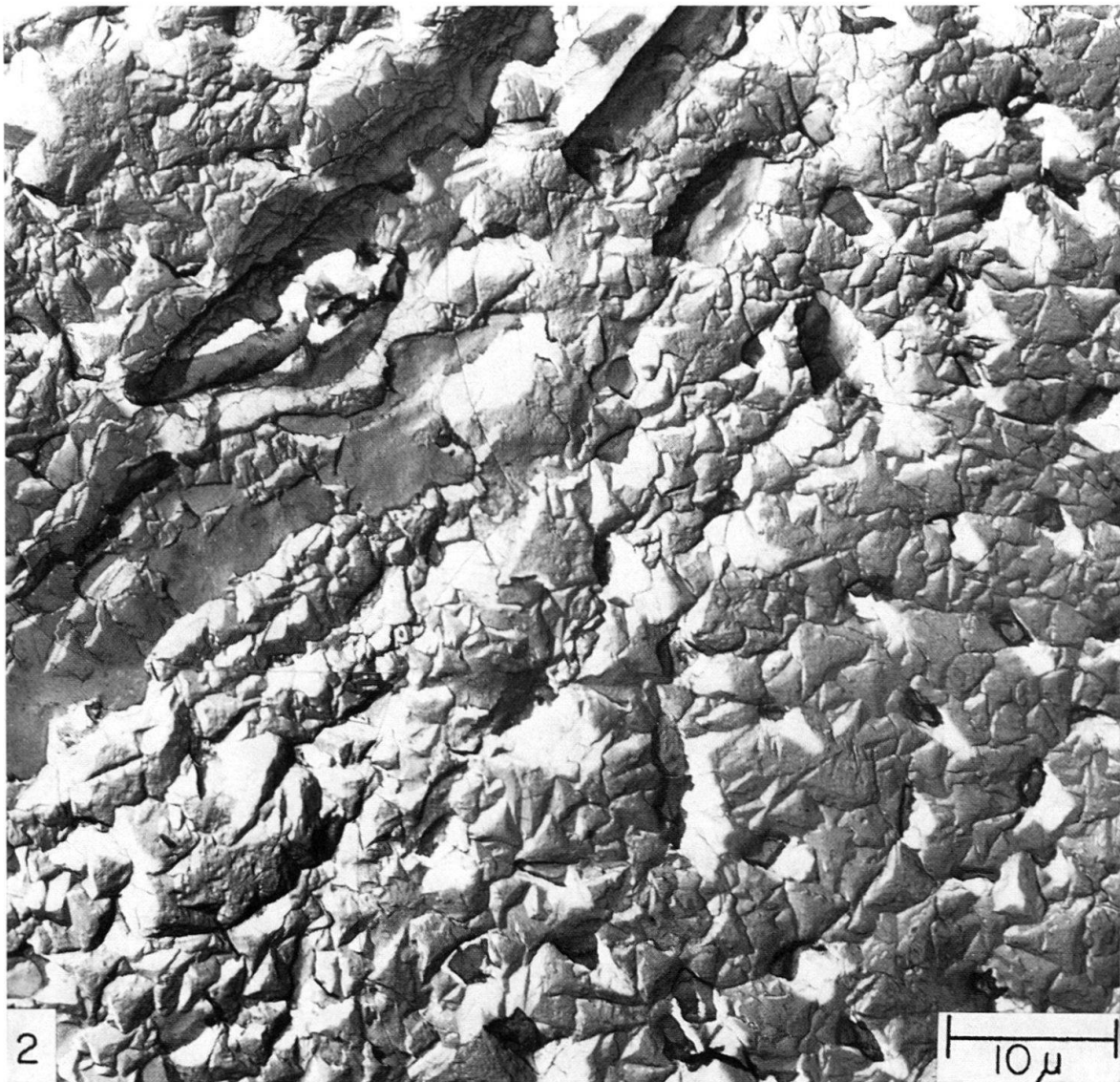
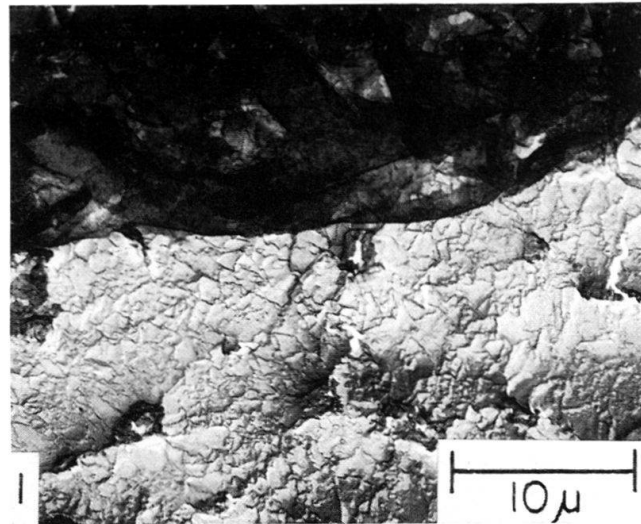


Plate VII

Fig. 1. Chamber 2. Crystals are larger than those of Chamber 3, thus further obscuring the pores (arrows). Part of keel is visible at bottom (Square 35 in Plate II).

Fig. 2. Chamber 2. Maximum crystal growth in the umbilical-apertural region has obliterated the pores. The very large crystals or crystal aggregates in the upper left are «pustules» (Square 33 in Plate II).

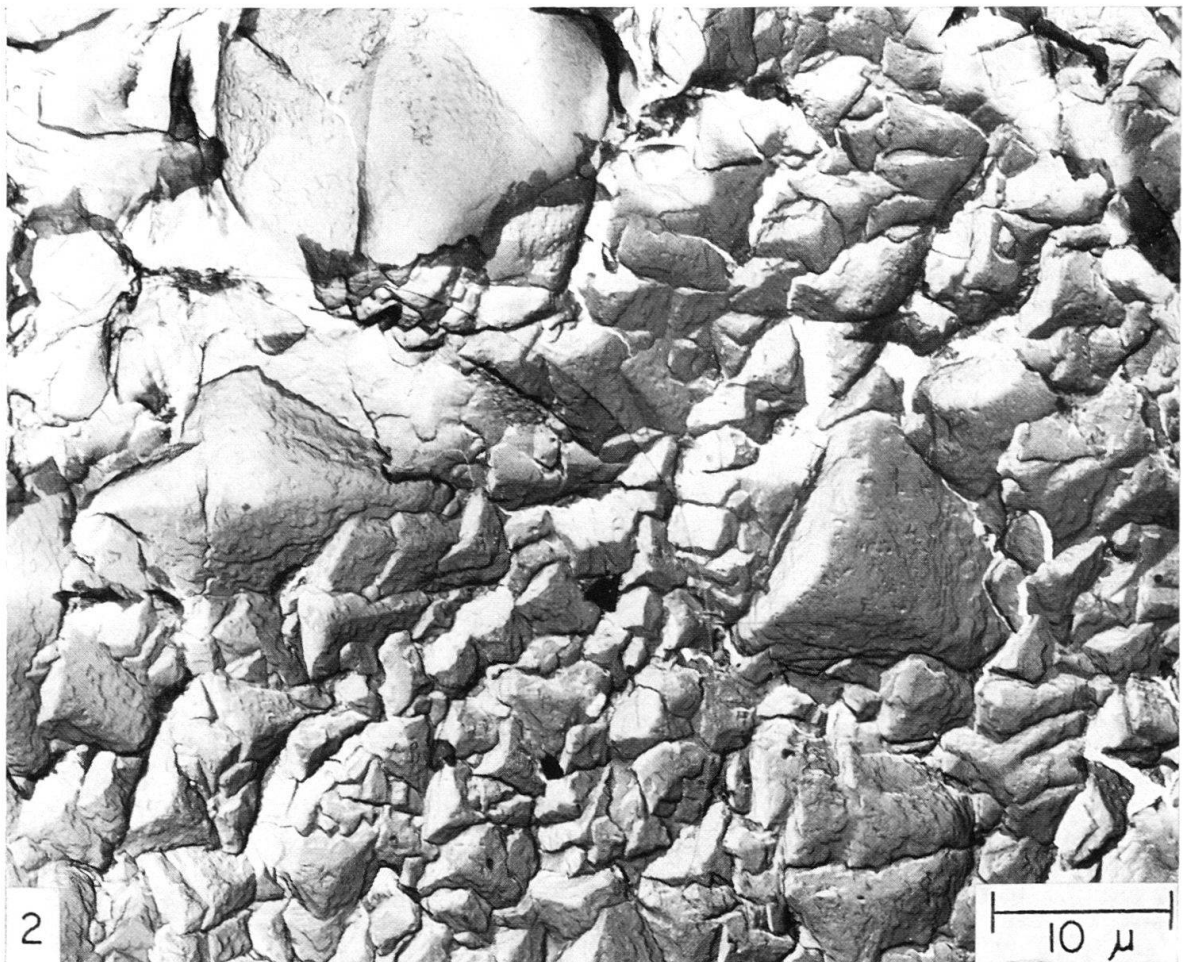
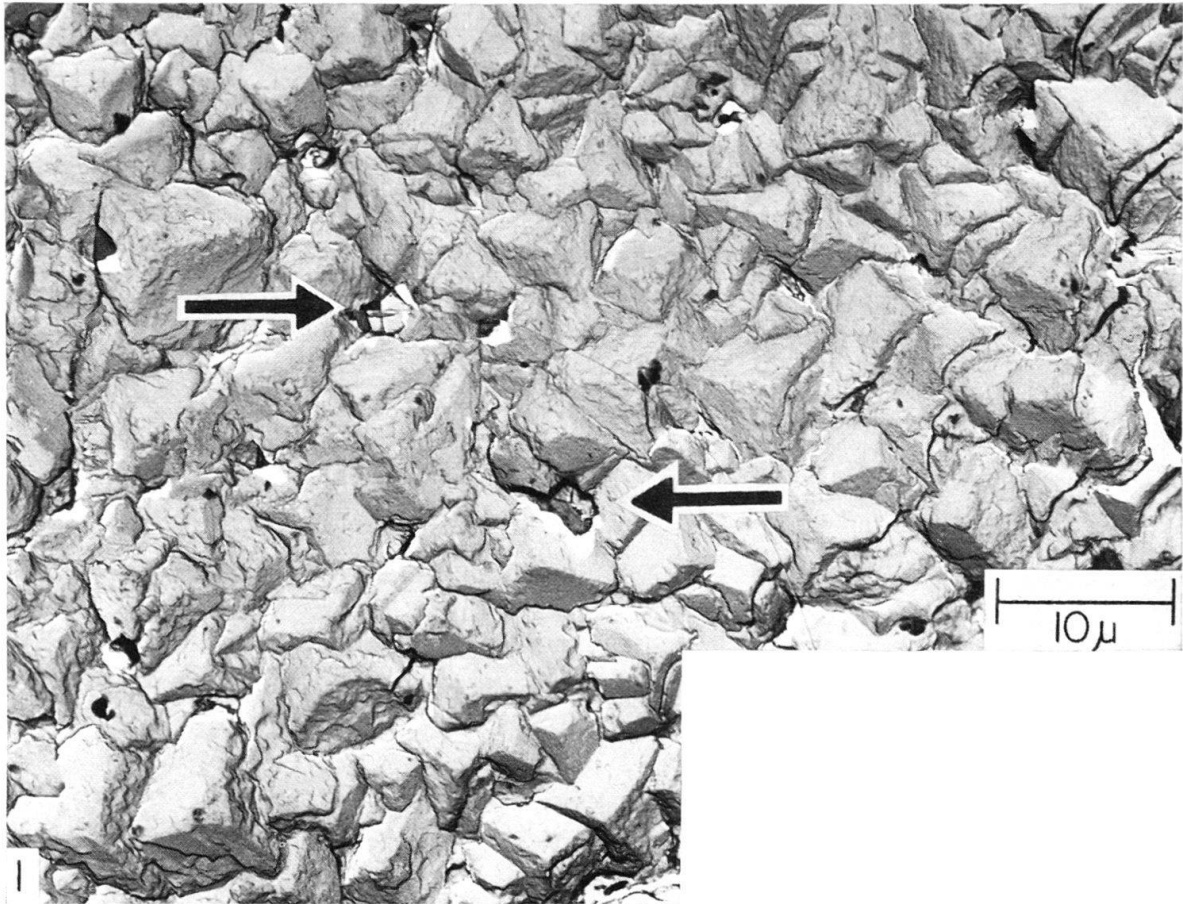
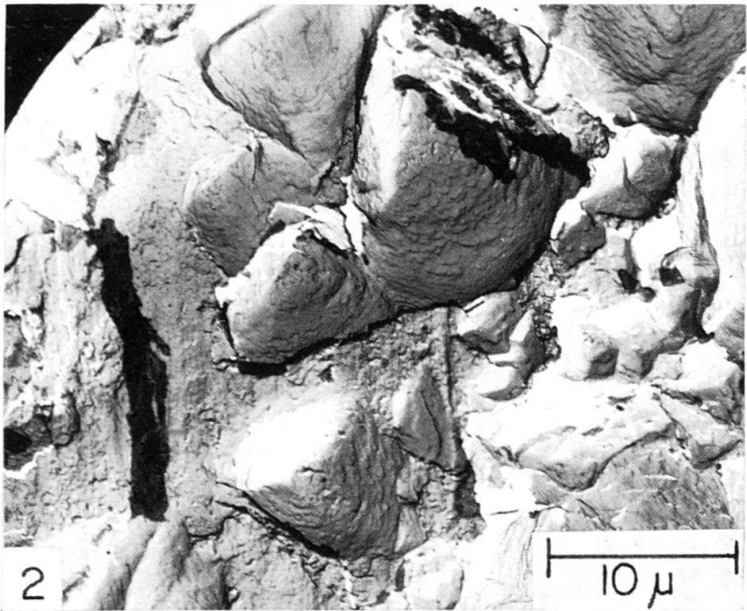
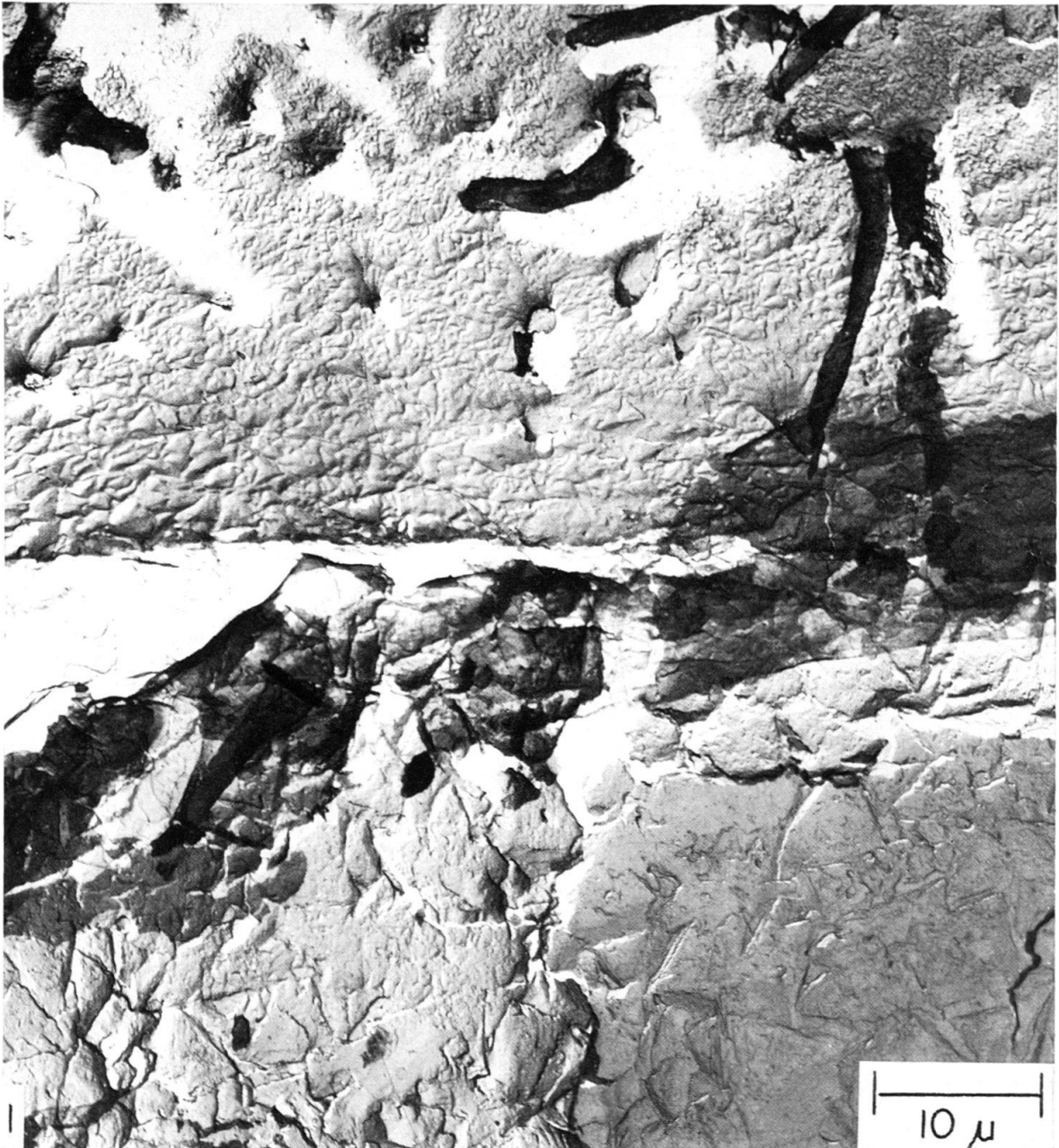


Plate VIII

Fig. 1. Apertural lip on Chamber 5. Pores in upper part grade into transition region with small rhombic crystals. The lip itself (bottom half) is composed of larger crystals (Square 21 in Plate II).

Fig. 2. Chamber 1 near umbilical-apertural region where large crystals appear as pustules (Square 25 in Plate II).



Selected electron-micrographs of *G. menardii*'s keel from various specimens prepared by direct-replica method. All views on Plates IX–XI are from apertural sides, except Plate XI, Fig. 2, which is from the spiral side.

Plate IX

Fig. 1. Keel on Chamber 5. Note that the microcrystals are oriented in 3 preferred directions, as in lower left, which form the bases for rhombic crystal growth. The oval structure in right of center is a coccolith.

Fig. 2–3. Keel on Chamber 5 with parallel ridges and early stages of crystal development.

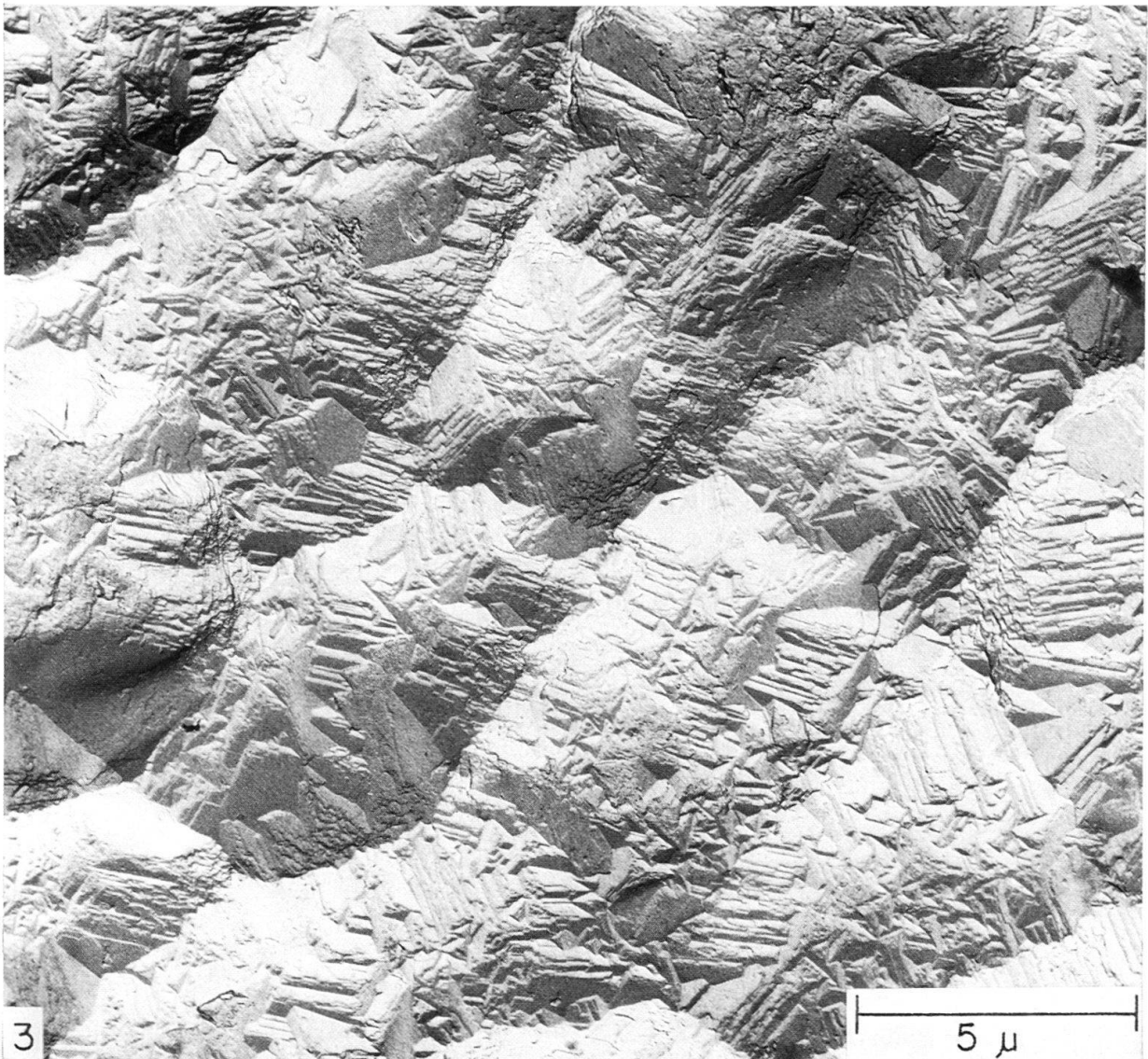
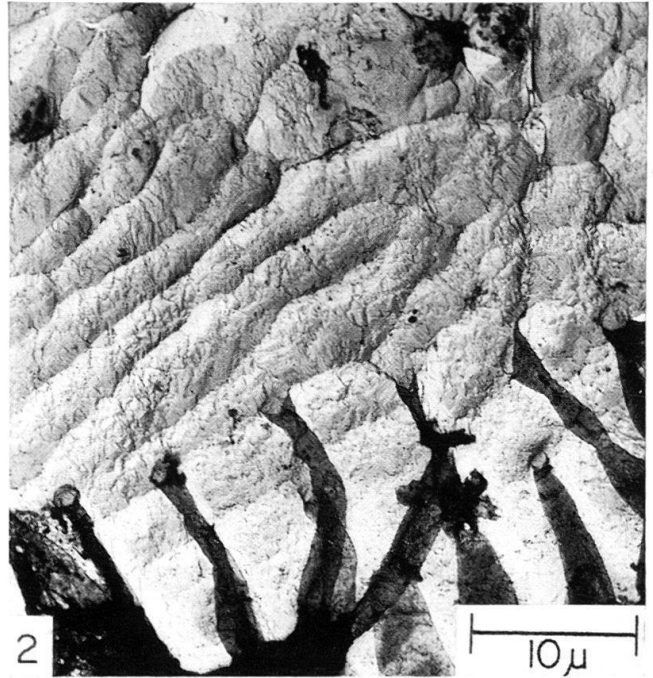
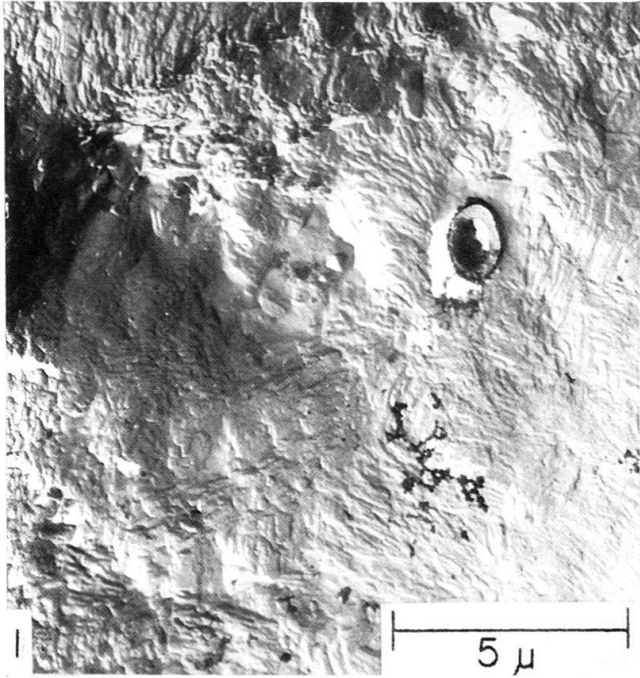


Plate X

Figs. 1, 2, and 3. Keel on Chamber 4 (Fig. 1) and Chamber 3 (Figs. 2 and 3), respectively. Further crystal growth is evident in the formation of larger structural units (knobs, papillae, pustules), made of crystal aggregates whose faces display many growth steps.

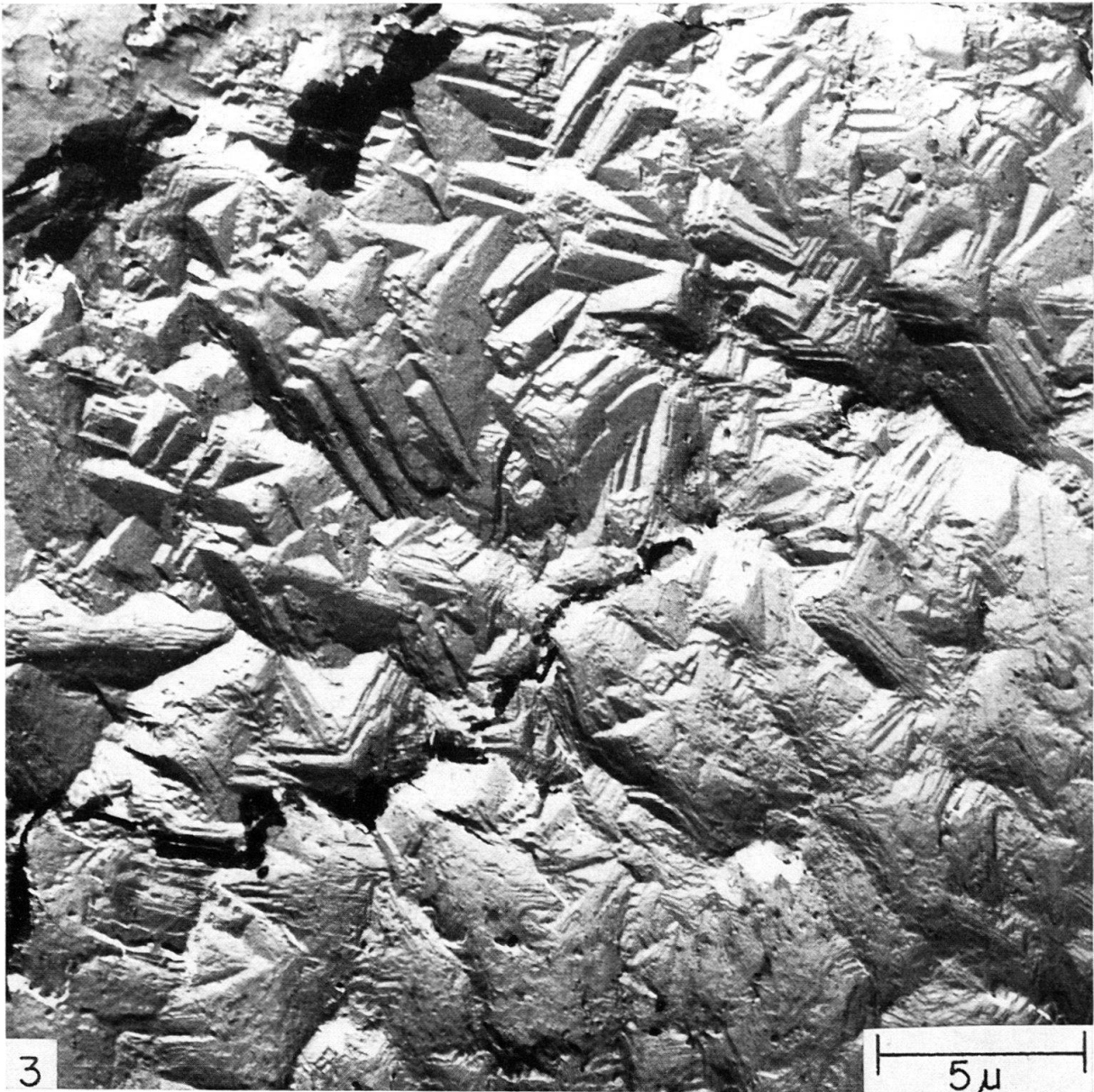
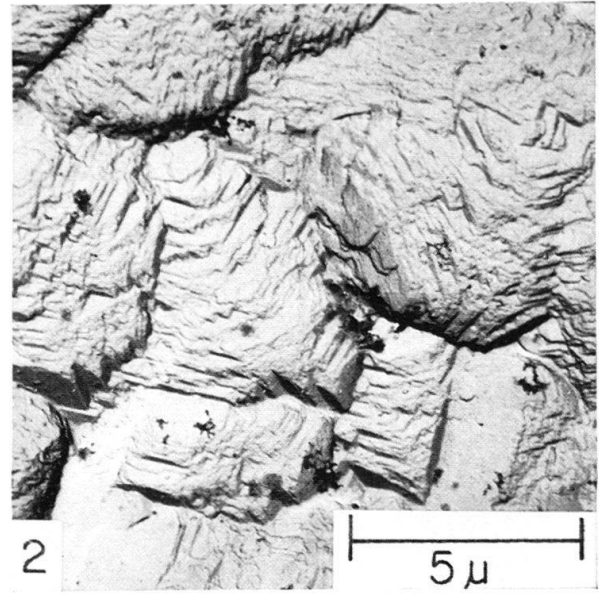
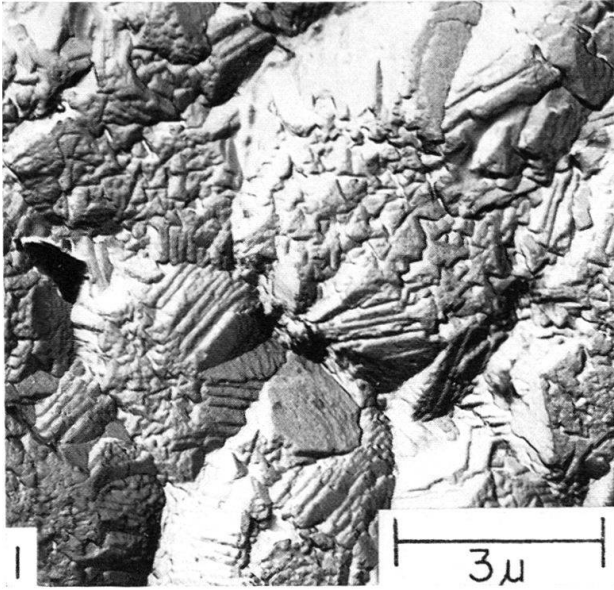
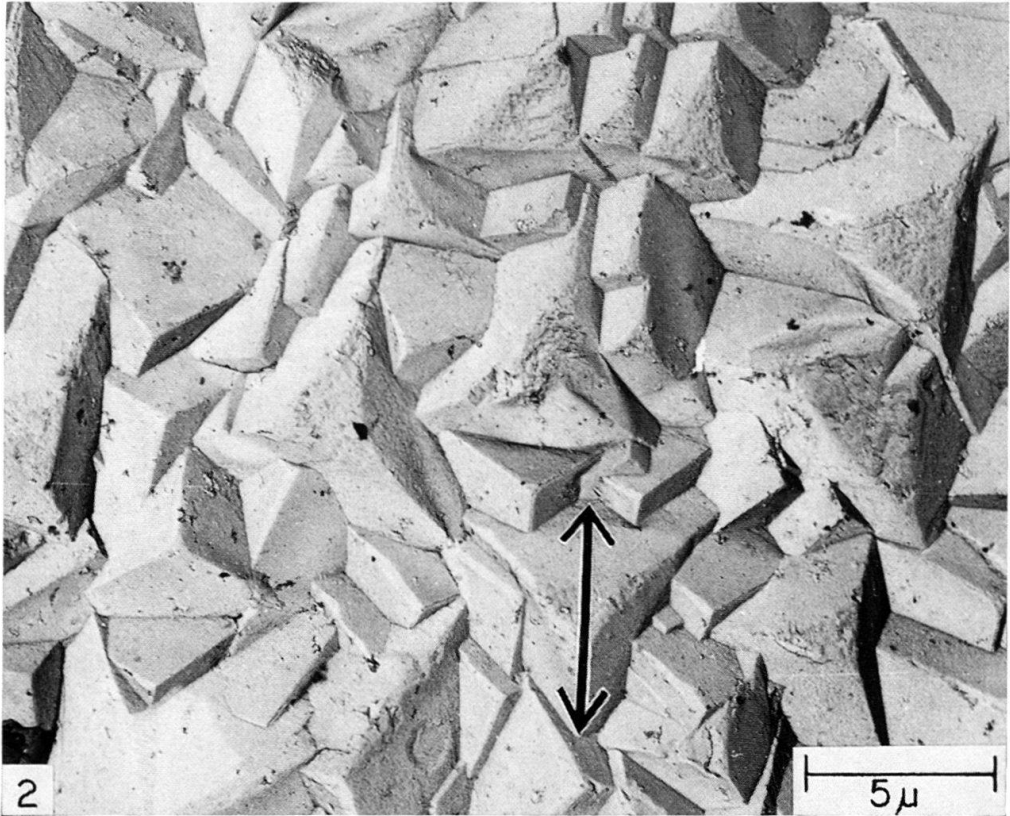
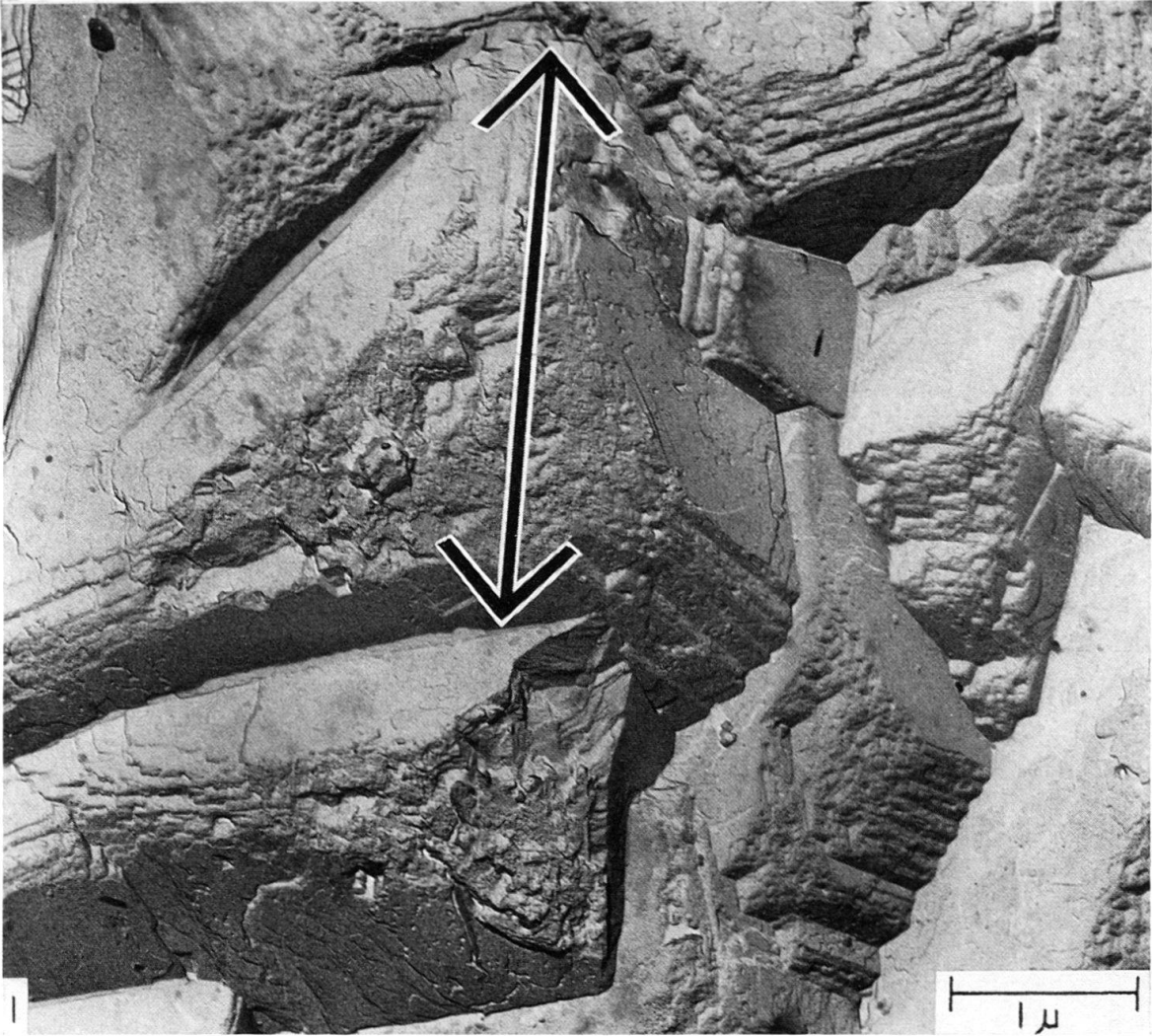


Plate XI

Fig. 1. Keel on Chamber 2. The large, euhedral calcite crystals are nearly completed, as deduced from the smooth faces and few remaining growth steps. Crystal size is measured from one end of the intersection of two faces to the base of the third face (double-pointed bars in Figs. 1 and 2).

Fig. 2. Keel on spiral side of Chamber 1. Ultimate crystal growth is attained, as inferred from the maximum crystal size and perfectly smooth faces of the euhedral, rhombic crystals.



Selected electron-micrographs of *G. menardii*'s chambers from various specimens prepared by direct-replica method. All views on Plates XII–XIV are from apertural side.

Plate XII

Fig. 1. Four pores on Chamber 5. Note concentric depressions surrounding the rims and the microcrystals making up the interpore region.

Fig. 2. Chamber 5 with pores of approximately equal diameters and smooth interpore region. Pore concentration: about 13 pores per $25 \times 25 \mu$ area.

Fig. 3. Chamber 5 close to keel, where the pores are of two sizes. Large pores are rimmed by circular depressions.

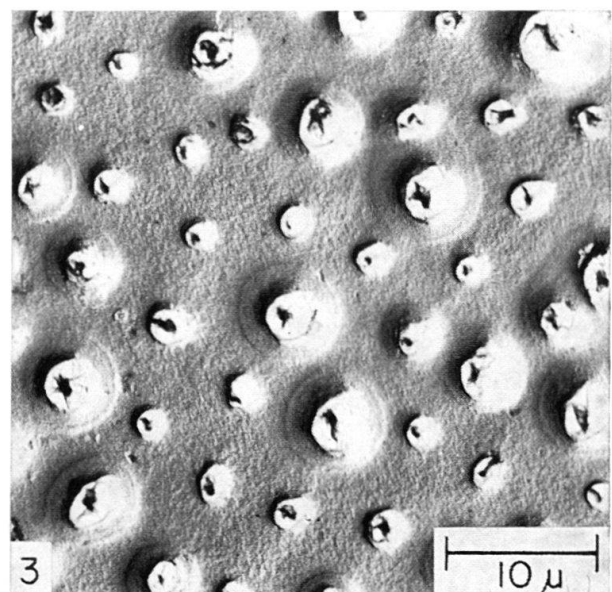
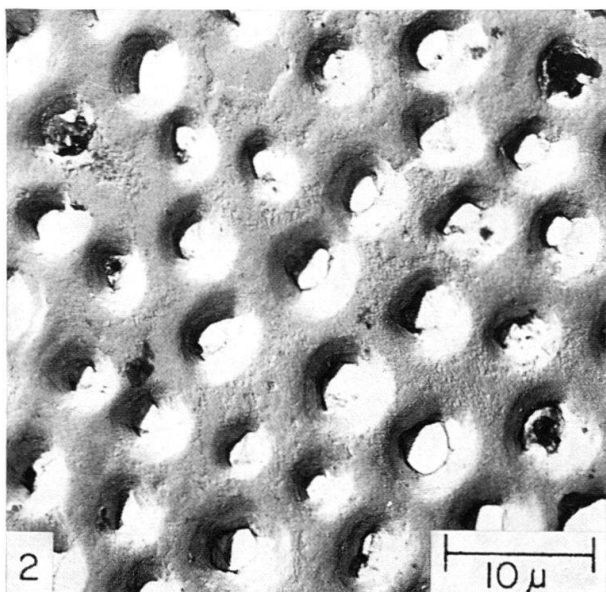
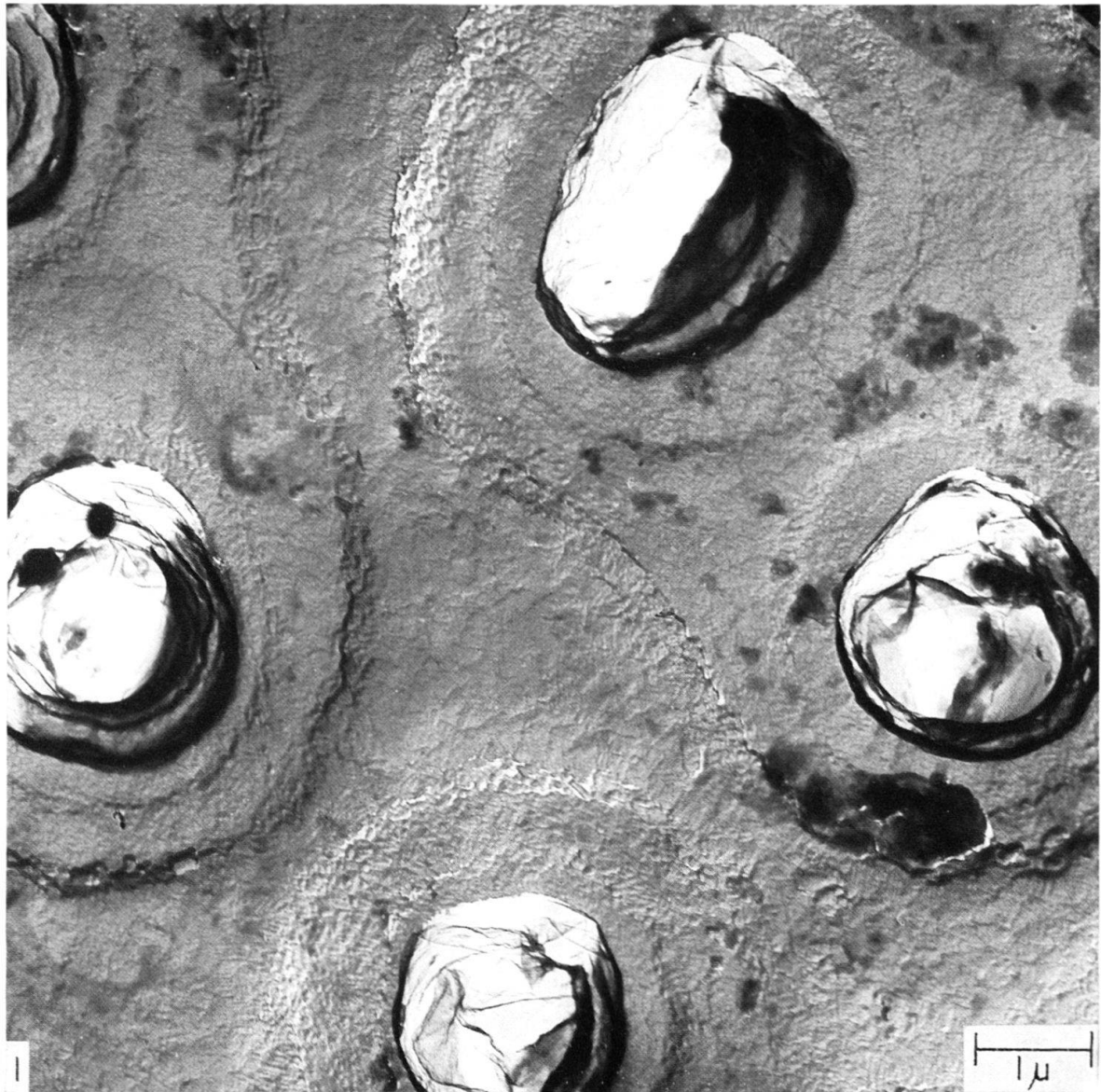


Plate XIII

Fig. 1. Chamber 4 showing transition from keel (left) to porous chamber (right). Note the oblique trend of linear ridges and the reduction of pore diameters near the keel.

Fig. 2. Chamber 4 close to keel. Pores are somewhat constricted by growth of parallel ridges.

Figs. 3-4. Same as Fig. 2, at higher magnifications.

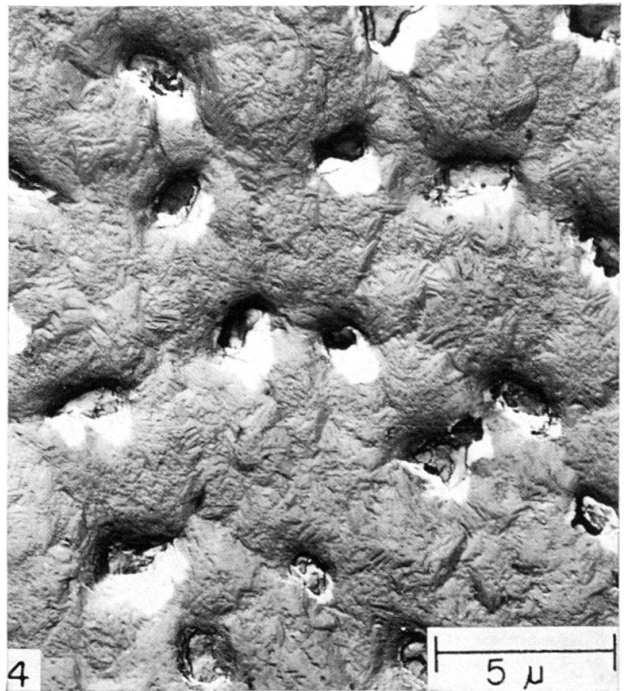
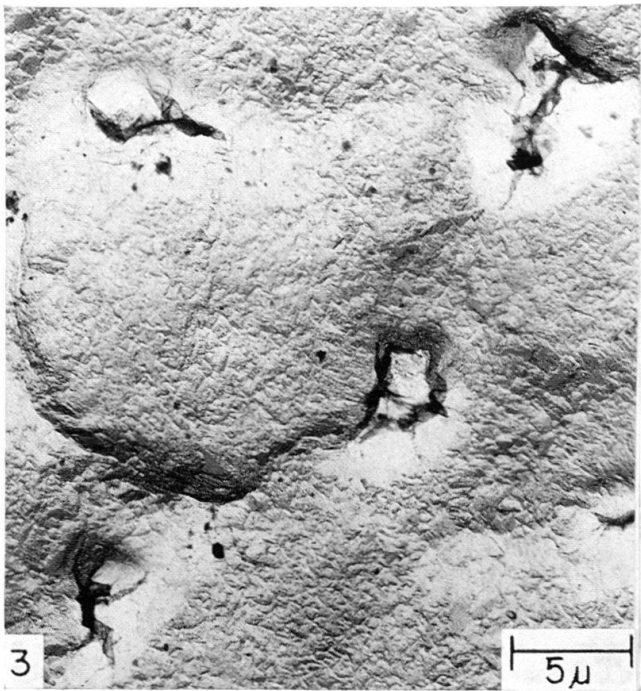
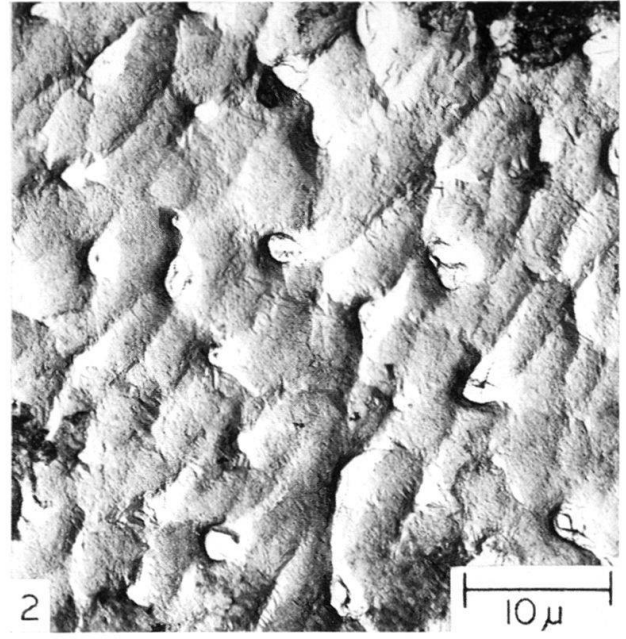
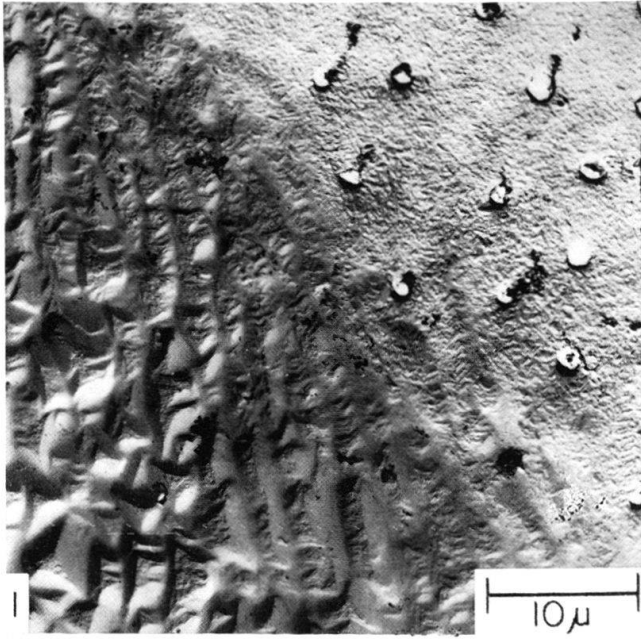


Plate XIV

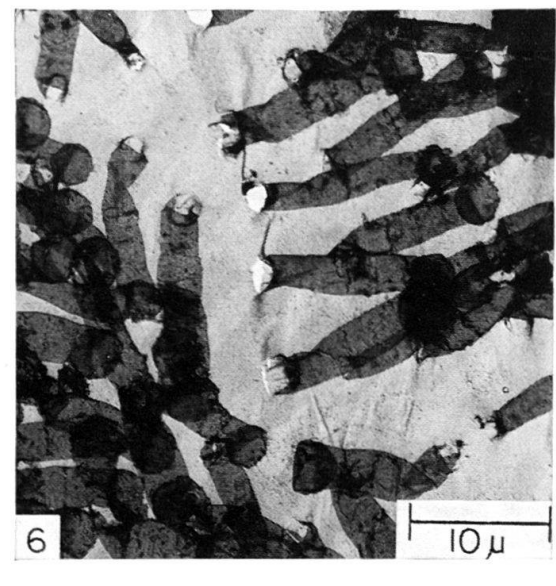
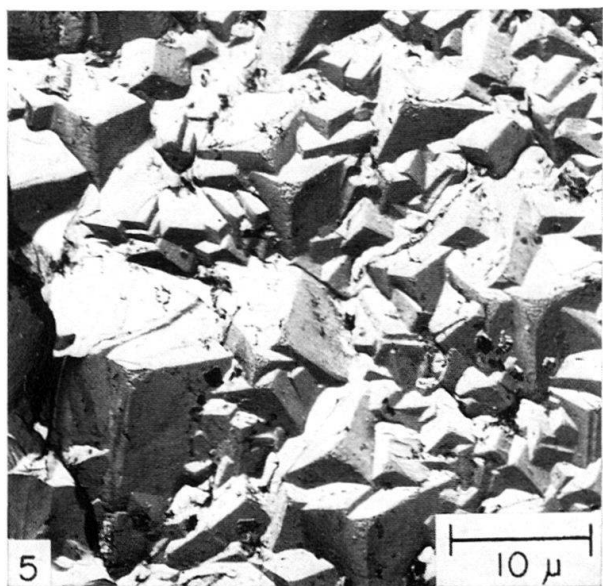
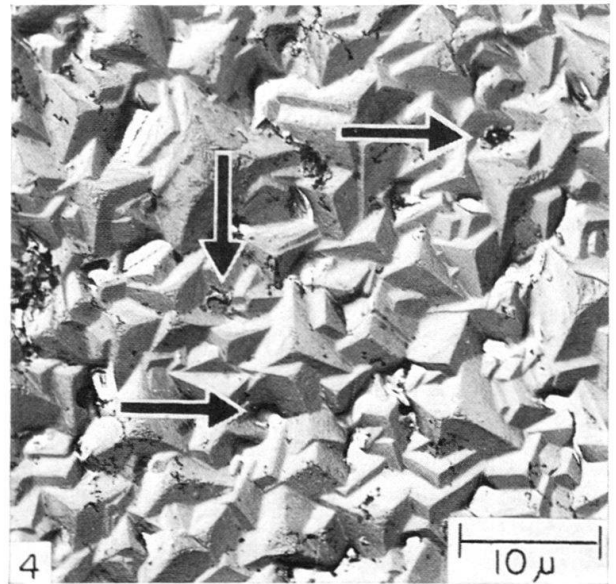
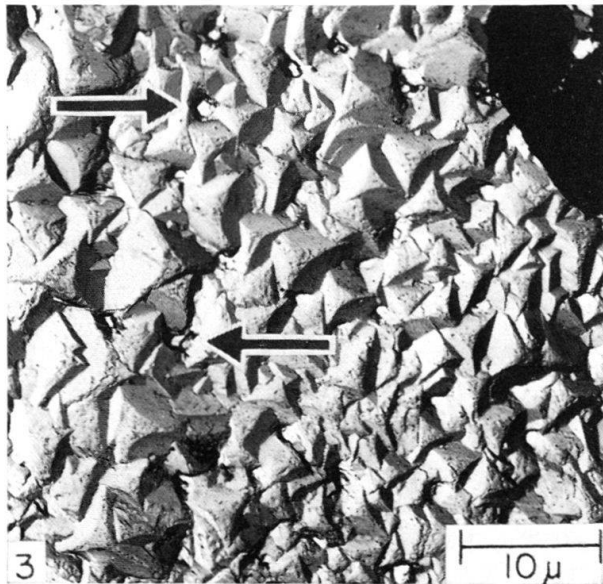
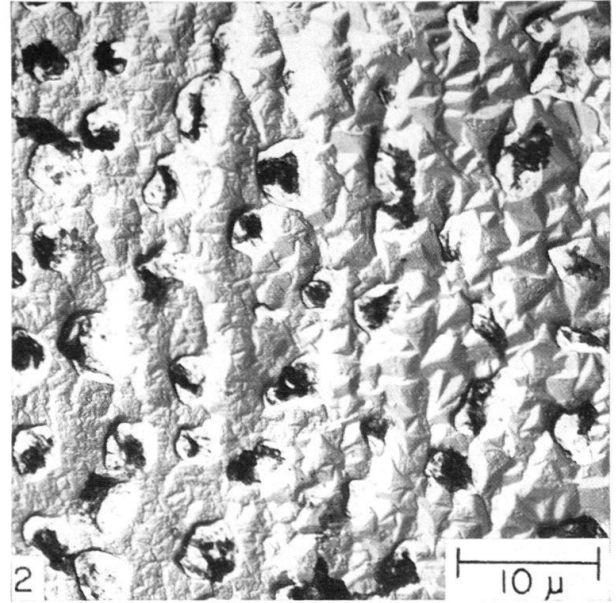
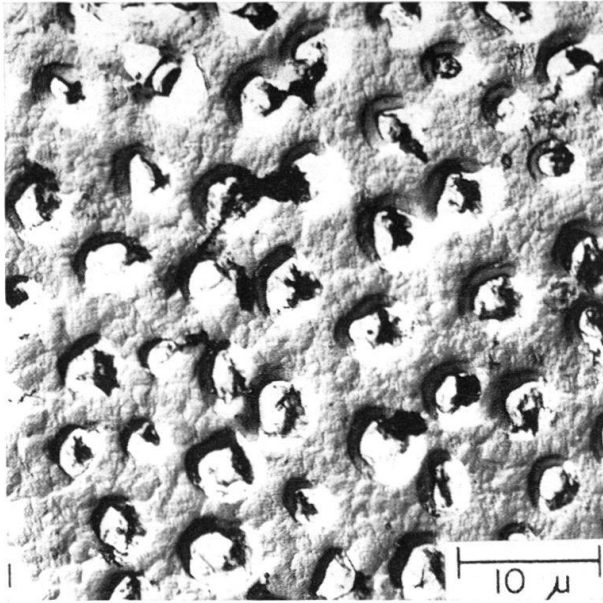
Fig. 1. Chamber 4 with large pore openings and beginning of crystalline thickening of interpore region. There are still about 13 pores per $25 \times 25 \mu$ area.

Fig. 2. Chamber 3 with two zones of varying crystal sizes. Pore concentration is about the same as in Chamber 4, although the pore diameters are smaller.

Figs. 3–4. Chamber 2. With further growth, the coarse rhombic crystals are choking off or greatly constricting the pores (arrows). Note that the pores are generally bounded by the bases of 3 or 4 crystals.

Fig. 5. Chamber 1 below aperture. Maximum growth of calcite crystals occurs here and pores are completely obliterated.

Fig. 6. Pore tubes that are replicated by the two-stage process and which subsequently have fallen on top of the surface replica. Pores average 12μ in length and 2μ in diameter.



Selected electron-micrographs of the spiral side of *G. menardii* on Plates XV–XVII.

Plate XV

Fig. 1. Pores on Chamber 5.

Fig. 2. Keel with parallel ridges trending obliquely to the periphery of the chamber. The pore tubes replicated in the two-stage process give an indication of their shape and size.

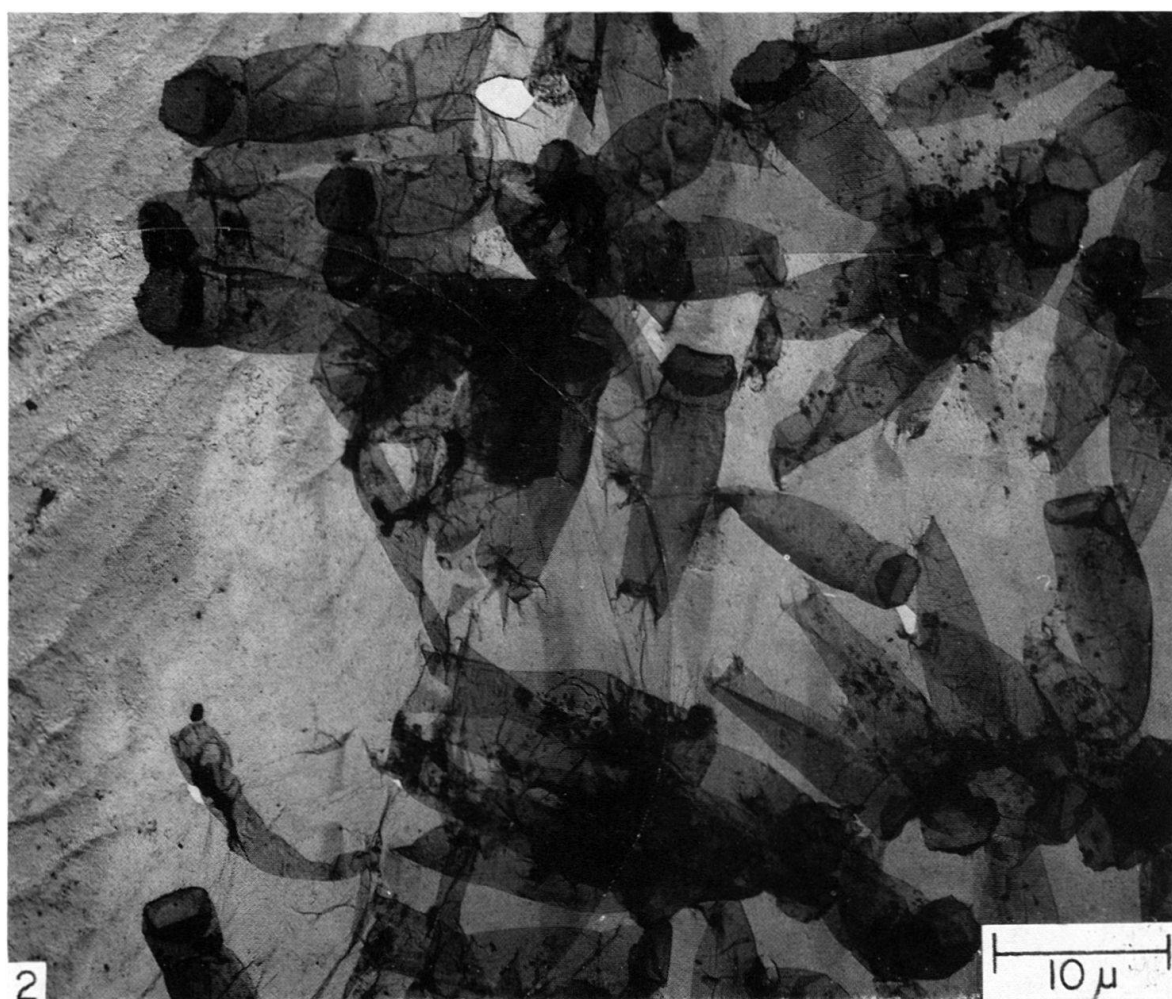
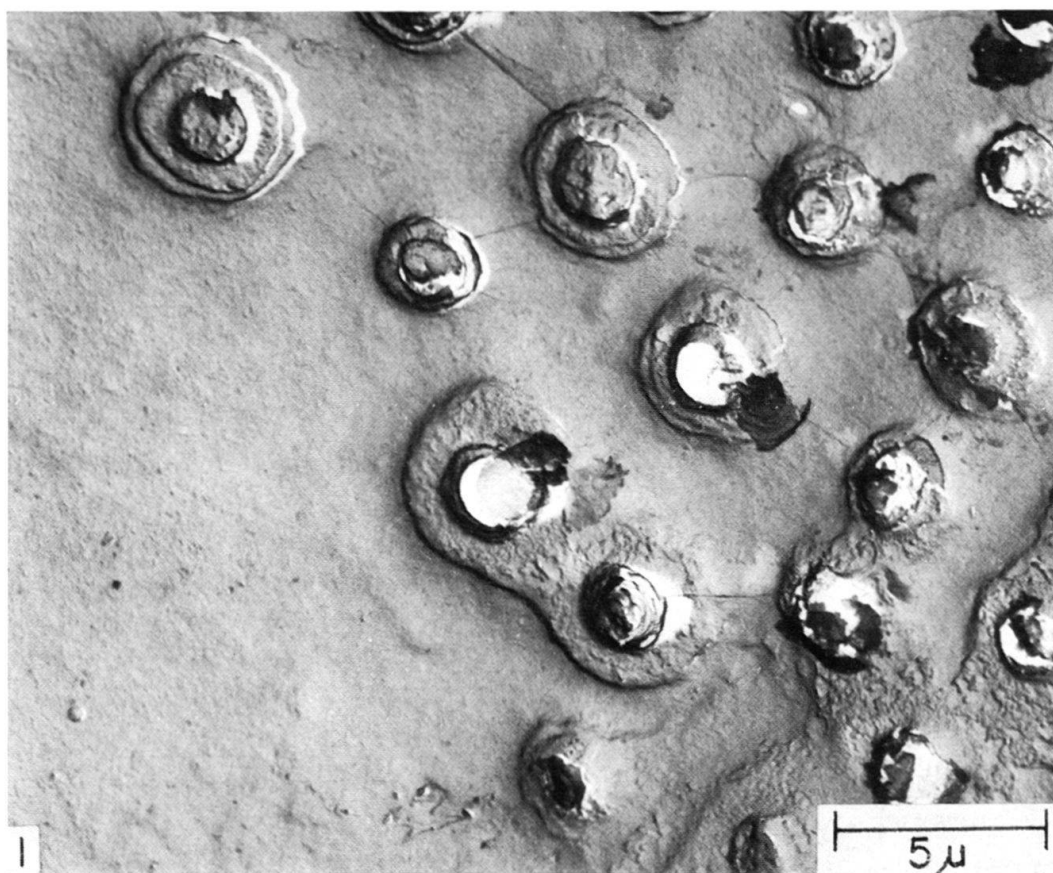


Plate XVI

Fig. 1. Pores on Chamber 4 and septal keel with parallel ridges between Chambers 4 and 5.

Fig. 2. Chamber 3 with zones of different crystal sizes.

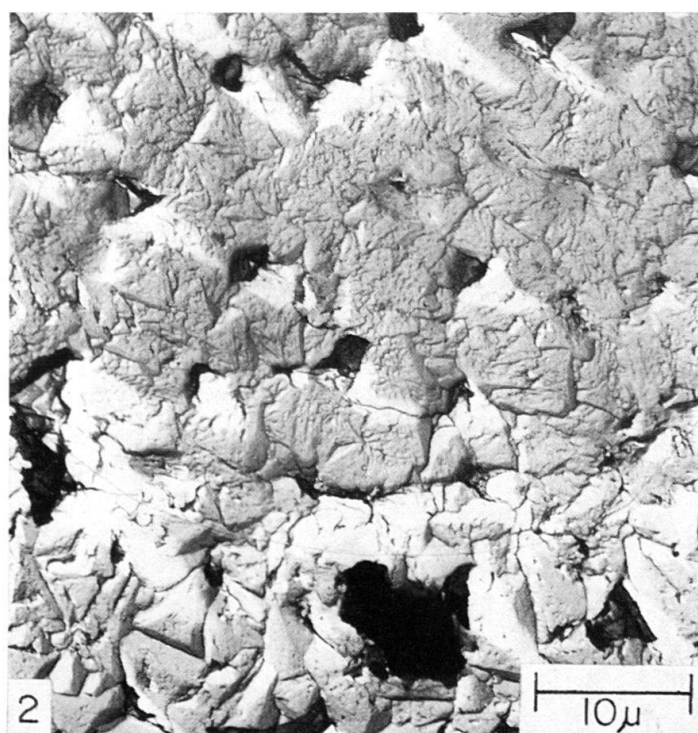
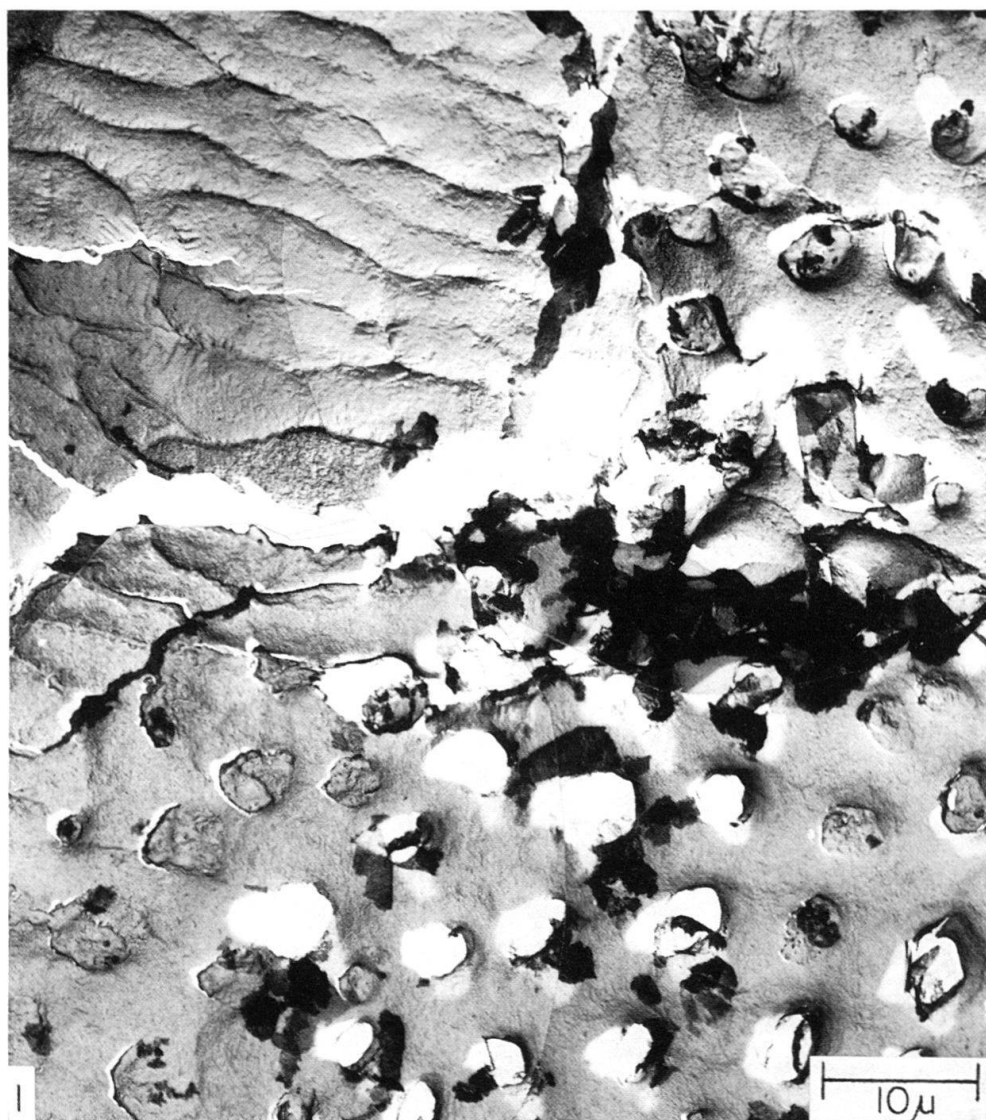


Plate XVII

Fig. 1. Keel on Chamber 4, showing a zone of parallel ridges near the edge of the chamber (right) and more massive structures trending perpendicular to the shell periphery.

Fig. 2. Cross section of test wall, showing radial-columnar structure and the outer (o) and inner (i) surfaces of the test.

